学位論文
Doctor's Thesis

Analysis of the RNA polymerase 1-2 gene mutant mouse line established by gene trapping

（遺伝子トラップ法により樹立された RNA polymerase 1-2 遺伝子変異マウスの解析）

陳 輝

Hui Chen

熊本大学大学院医学教育部博士課程生体医科学専攻神経発生学

指導教員

大久保 博晶 前教授

熊本大学大学院医学教育部博士課程生体医科学専攻神経発生学

山村 研一 教授

熊本大学大学院薬学教育部博士課程生命薬科学専攻臓器形成学

紹介教授

山本 哲郎 教授

熊本大学大学院医学教育部博士課程病態制御学専攻分子病理学

2008年3月

学　位　論　文

Doctor's Thesis

論文題名： Analysis of the RNA polymerase 1-2 gene mutant mouse line established by gene trapping
（遺伝子トラップ法により樹立されたRNA polymerase 1-2 遺伝子変異マウスの解析）

著 者 名 ： 陳 輝
Hui Chen

指導教員名 ：熊本大学大学院医学教育部博士課程生体医科学専攻神経発生学　大久保　博晶前教授
熊本大学大学院薬学教育部博士課程生命薬科学専攻臓器形成学　山村　研一教授

審査委員名 ： 医学教育部　器官制御分野学担当教授　中尾　光善
医学教育部分子遺伝学分野学担当教授　尾池　雄一
医学教育部幹細胞制御分野学担当教授　粂　昭苑
医学教育部　初期発生分野学担当教授　永渕 昭良

２００８年３月

CONTENTS

要旨

リボゾームRNA（rRNA)の生合成は、細胞の増殖・分裂と密接に関連しており、細胞生物学的に最も普遍的かつ重要な機能の一つである。rRNAはRNA合成酵素Ⅰ（RNA PolI)によって転写される。この機能が阻害されることにより、マウスの発生分化にどのような影響が生じるかを研究するため、RNA PolIの構成タンパクの中で2番目に大きいサブユニットをコードする*Rpo1-2*遺伝子内に遺伝子トラップベクターが挿入された挿入変異マウスを用い、その解析を行なった。*Rpo1-2*遺伝子は15個のexonより構成されているが、トラップベクターは、14番目のexon内に挿入されており、挿入に伴う大きなゲノムの欠失などは見られなかった。トラップアレルの転写産物の解析から、全長1135aaのうちC末側312aaを欠失したRpo1-2タンパクが産生されると予測された。ホモ接合体は7.5日胚でも存在せず、吸収された胚も見られなかったため、着床前致死が示唆された。そこで、着床前の胚を*in vitro*で培養し、形態観察及び個々の胚の遺伝子型を解析した結果、ホモ胚は、桑実胚まで外見上正常に発生し、その後変性して致死に至ることがわかった。ホモ胚では、桑実胚の段階ですでにrRNA合成が著しく低下しており、核小体の構造も失われていた。また、変性しているホモ胚はterminal deoxynucleotidyl transferase mediated dUTP nick end labeling（TUNEL)染色陽性であったことから、アポトーシスにより死亡していると考えられた。以上の結果より、*Rpo1-2*遺伝子のC末側約４分の１の欠失で、RNA polI活性はほとんど失われたと考えられ、また、rRNA合成の停止が核小体の破壊を引き起こし、その結果、アポトーシスが誘導されるシステムが働いたと考えられる。

Summary

Ribosomal biogenesis is closely involved in cell growth and proliferation. Ribosomal RNA gene (rDNA) transcribed by RNA polymerase I (Pol I) is an important initial step for production of ribosomes. The *RNA polymerase 1-2 (Rpo1-2)* gene is comprised of 15 exons and encodes 1135 amino acids (aa) of the second largest subunit in Pol I. In a gene trap screen using pU-Hachi vector carrying the *IRES-βgeo*, we have identified an insertion mutation in the *Rpo1-2* gene ($Rpo1\text{-}2^{Gt}$). The trap vector was inserted into the 14th exon, resulting in a truncation of 312aa from the C-terminus. $Rpo1\text{-}2^{Gt/Gt}$ homozygous embryos were not found at 7.5dpc, and no resorption site was observed in the uteri of heterozygous intercrosses females, which means the $Rpo1\text{-}2^{Gt/Gt}$ embryos died around preimplantation stage. We collected embryos from heterozygous intercrosses at the 2-cell stage, observed their growth in culture till the blastocyst stage. $Rpo1\text{-}2^{Gt/Gt}$ embryos were initially indistinguishable from wild type and $Rpo1\text{-}2^{Gt/+}$ embryos until the morula stage. Then all $Rpo1\text{-}2^{Gt/Gt}$ embryos failed to form a normal blastocoel and inner cell mass (ICM), and became progressively more disorganized and fragmented with extensive cellular degeneration. In $Rpo1\text{-}2^{Gt/Gt}$ embryos, the synthesis of rRNA was severely impaired and they displayed nucleolus disruption at morula stage. Terminal deoxynucleotidyl transferase mediated dUTP nick end labeling (TUNEL) stain showed $Rpo1\text{-}2^{Gt/Gt}$ embryos died of apoptotic cell death. These results indicate that the loss of rDNA transcription induced nucleolar structure disorganization and apoptosis in preimplantation embryos.

Publication list

Chen, H., Li, Z., Haruna, K., Li, Z., Li, Z., Semba, K., Araki, M., Yamamura, K., Araki, K. Early pre-implantation lethality in mice carrying truncated mutation in the RNA polymerase 1-2 gene. ***Biochem. Biophys. Res. Commun.*** 365: 636-642, 2008.

Acknowledgements

I would like to thank Prof. Ken-ichi Yamamura who kindly gave me the precious opportunity to study in the Division of Developmental Genetics, Institute of Molecular Embryology and Genetics (IMEG), Kumamoto University.

I would like to thank Dr. Kimi Araki who is an associate professor in the Division of Developmental Genetics, Institute of Molecular Embryology and Genetics (IMEG), Kumamoto University, for giving me continuous supervision and valuable suggestion. I learned a lot about biological science from her.

I would like to extend my gratitude to Dr. Zhenghua Li, Ms. Kyoko Haruna, Ms. Yumi Sakumura, Mr. Koichiro Miike, Mr. Ryo Yamashita, Ms. Yuko Tsuruta, Dr. Mayumi Muta, Associated Prof. Masatake Araki for their kind help, friendly cooperation and valuable advice. I also thank Mrs. Michiyo Nakata for technical assistance such as immuno-histochemical work.

Finally, I would like to thank Mr. Qingbo Liu, my husband, and Xinran Liu, my daughter, who always help and support me to accomplish my scientific carrier.

Abbreviation

CF: core factor

CP: core promoter

DFC: dense fibrillar component

dpc: days post coitus

ECMV: encephalomyocarditis virus

ES cell: embryonic stem cell

ETS: external transcribed spacer

FC: fibrillar center

GC: granular component

hCG: human chorionic gonadotropin

hphCG: hour post hCG

ICM: inner cell mass

IRES: internal ribosomal entry site

ITS: internal transcribed spacer

LacZ: β-Galactosidase

mRNA: messenger RNA

NORs: nucleolar organizer regions

NP-40: Nonidet P-40

NPBs: nucleolar precursor bodies

PCR: polymerase chain reaction

PIC: pre-initiation complex

PMS: pregnant mare serum gonadotropin

Pol I: RNA polymerase I

Pol II: RNA polymerase II

Pol III: RNA polymerase III

RACE: Rapid Amplification of cDNA Ends

rDNA: ribosomal DNA

Rpo1-2: RNA polymerase I subunit 2

rRNA: ribosomal RNA

snRNPs: small nuclear ribonucleoproteins

TBP: TATA-binding protein factor

TdT : terminal deoxynucleotidyl transferase

TE: 10 mM Tris-HCl (pH 7.5)/1 mM EDTA

TIF-IA: transcription initiation factor IA

TIF-IB: transcription initiation factor IB

tRNA: transfer RNA

TUNEL: TdT mediated dUTP nick end labeling

UAF: upstream activating factor

UBF: upstream binding factor

UE: upstream element

X-gal: 5-bromo-4-chloro-3-indolyl β-D-galactopyranoside

βgeo: *β-galactosidase/neomycin-resistance fusion* gene

Introduction

Chapter 1: Gene trapping

Gene trapping is a method of randomly generating embryonic stem cells (ES cells) (Evans and Kaufman, 1981) with well-characterized insertional mutations. The mutation is generated by inserting a gene trap vector construct into an intronic or coding region of genomic DNA. Gene trap vectors contain a promoter-less reporter gene (the *βgeo* gene in Figure 1) that is preceded by a splice acceptor. The reporter tag is useful for further experiment in mice to analyze expression pattern of trapped genes (Stanford et al., 2001). The vectors are introduced into the ES cell genome, and upon integration into an endogenous gene, a fusion transcript between the endogenous gene and the reporter gene is produced (Fig. 1A, B). The cDNA sequence of the trapped (disrupted) gene is easily determined by rapid amplification of cDNA 5'-ends (5'RACE) and direct sequencing using primers specific for the reporter gene (Fig. 1D) (Frohman et al., 1988). Furthermore, genomic DNA flanking the integrated trap vector can easily be obtained by the plasmid rescue method (Fig. 1E). Although the insertion of the vector construct into a gene typically results in complete inactivation of the "trapped" gene (a null allele), this is not guaranteed. In some cases vector insertion can fail to inactivate a gene, lead to hypomorphic gene function, or result in a dominant negative phenotype. Generally, vector insertion close to the 5' end of a gene is more likely to create a null allele than insertion near the 3' end.

Mutant mouse lines can be established from gene trap ES cell lines through germline transmission (Fig. 2) (Bradley et al., 1984). In order to facilitate the production of chimeric mice, we use TT2 ES cells (Yagi et al., 1993) from which chimeric mice can be produced economically and efficiently through aggregation with morulae from outbred ICR

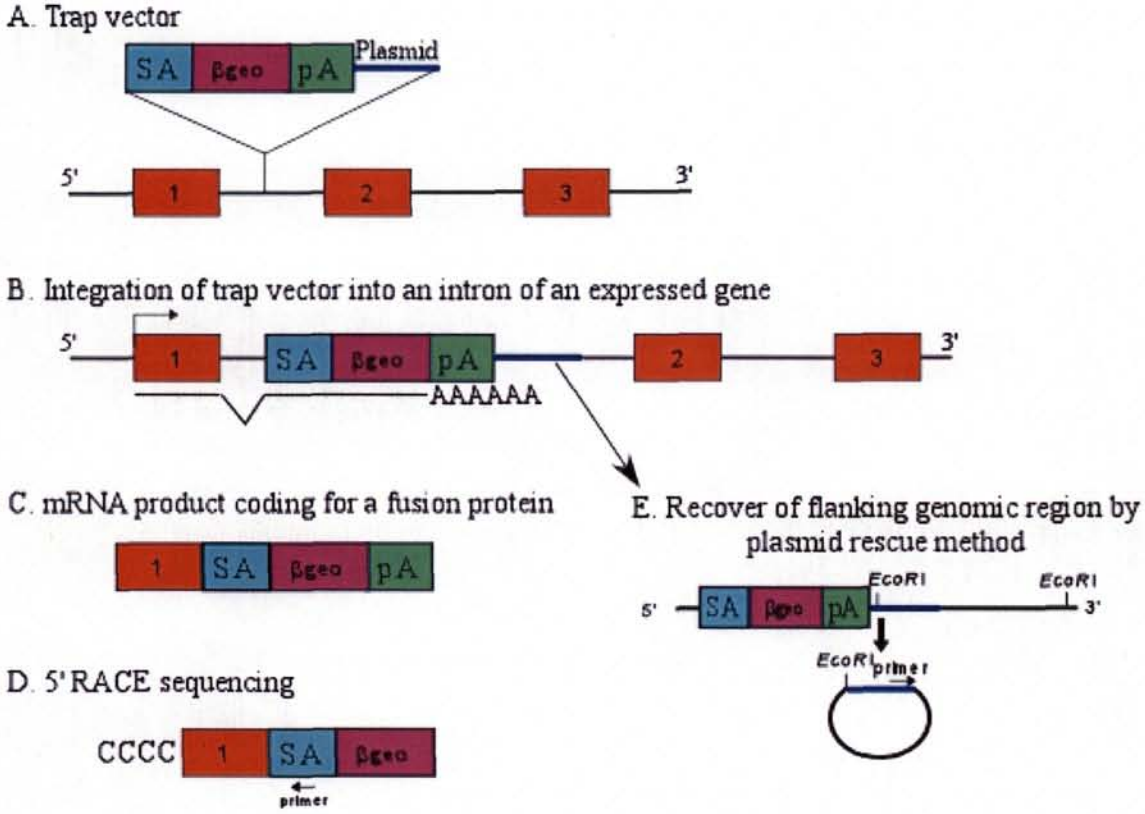

Figure 1. Modes of gene trap

(A) Gene trap vector random inserted into a genomic locus. (B) Integration of a vector into an intron of an expressed gene. (C) mRNA product coding for a fusion protein. Transcription of the integrated gene results in a truncated mRNA that will translate into a selectable, tagged protein. (D) 5' RACE sequencing. Primers that bind with the trap cassette are used to sequence the mRNA product in the 3' to 5' direction. (E) Plasmid rescue. Primers that bind with the trap cassette are used to sequence the integrated genomic sequence. Exons are indicated in numbers.

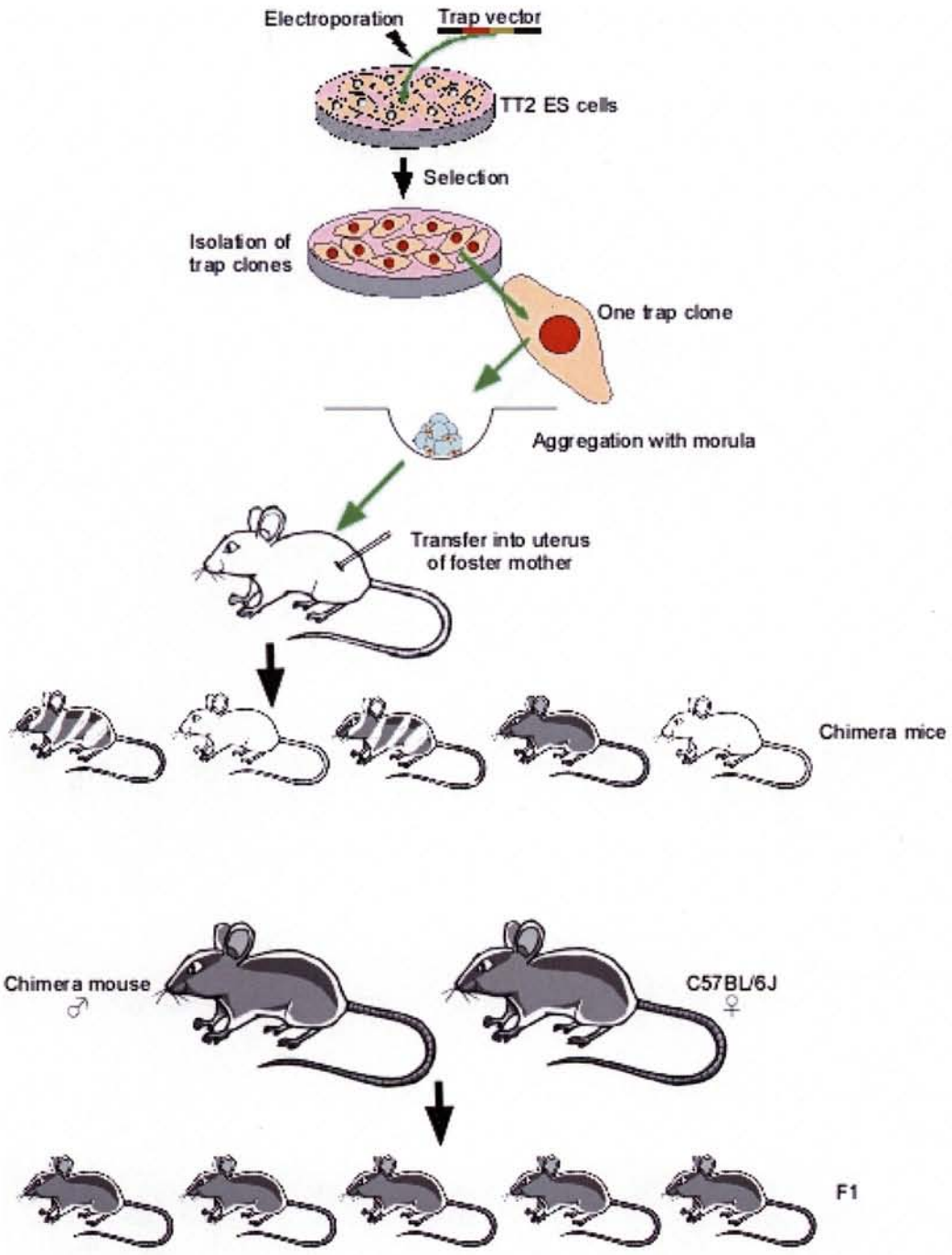

Figure 2. Germline transmission and establishment of trap mouse line.

mice. After germline transmission, gene trap lines can be analyzed for mutant phenotypes and also for the expression patterns of trapped genes which can be traced by simple histochemical staining of the reporter gene (usually β-galactosidase of *E. coli* is used).

There are a variety of different gene trap vector types, and each will produce cell lines with different characteristics and research opportunities. To date, trap vectors carrying the *β-galactosidase/neomycin-resistance fusion* gene (*βgeo*) (Friedrich and Soriano, 1991; Voss et al., 1998) have been widely used and proven to trap various genes expressed in ES cells (Bonaldo et al., 1998; Chowdhury et al., 1997; Stoykova et al., 1998). The internal ribosomal entry site (IRES) from the encephalomyocarditis virus (ECMV) (Ghattas et al., 1991; Jang and Wimmer, 1990; Kang et al., 1997; Mountford and Smith, 1995) is also frequently used in gene trap vectors to increase the efficiency of gene trapping. Since ribosomes are recruited to IRES and start translation from the AUG codon of the *βgeo* positioned downstream of IRES, the presence of an IRES in gene trap vector ensures the reporter and resistance activity without requiring an in-frame fusion with the coding region of the endogenous gene. In other words, trap clones can be obtained independently of the insertion sites of trap vector within trapped genes.

We have constructed an exchangeable gene trap vector, pU-Hachi, carrying SA-*lox*71-IRES-*βgeo*–polyadenylation signal (pA)-*lox*P-pA-pUC (Araki et al., 1999b), electroporated the linearized pU-Hachi vector into TT2 ES cells and isolated 109 trapped clones. In this study, we analyzed Ayu8019 clone in which the *Rpo1-2* gene was trapped.

Chapter 2: ribosomal RNA and RNA polymerase I

Ribosomes are macromolecular structures composed of ribosomal RNA (rRNA) bound to proteins. They exist in the cell cytoplasm, bind to mRNA and translated it to produce protein.

rRNA accounts for ~60% of the ribosome by weight and contributes directly to the catalytic processes of protein synthesis (Moore and Steitz, 2002).

Cells contain large numbers of ribosomes which must be replicated when the cell divided. As a result, cells have a huge requirement for rRNA which is produced by transcription of rRNA gene (rDNA) by RNA polymerase. To ensure that correct numbers of each of the different rRNAs are produced, the sequences of the 28S, 18S and 5.8S rRNAs are present in a single gene which exists as multiple copies separated from each other by short nontranscribed regions in eukaryotes (Fig. 3A). In mouse, there are about 100 genes per haploid genome arranged on three separate chromosomes (Long and Dawid, 1980). The genes are transcribed by RNA polymerase I (Pol I) in the cell nucleus in a region known as nucleolus. During mitosis the genes for preribosomal RNA (pre-rRNA) are usually localized to secondary constrictions of chromosomes. They have the ability to initiate the formation of nucleoli during interphase; hence, they are called nucleolus organizer regions or NORs (Olson et al., 2002). rRNAs are transcribed as a single, large 45S pre-rRNA and undergone a series of process to form mature 28S, 18S and 5.8S rRNAs (Fig. 3B). The 5S rRNA is transcribed separately by the RNA_polymerase III (Pol III) from unlinked gene which does not undergo processing.

Fifty percent, or more, of RNA synthesis, in a rapidly proliferating eukaryotic cell, is expended on rDNA transcription (Moss, 2004). Ribosome biogenesis is a high energy and nutrient consuming process; therefore, there is a fine balance between the growth status of the cell and the accumulation of rRNAs. In responding to changes in environmental conditions, the rate of Pol I transcription is changed to control ribosome production and the potential for cell proliferation. Efficient transcription of rDNA by Pol I requires the formation of a pre-initiation complex (PIC) on the promoter, including upstream activating factor (UAF) and

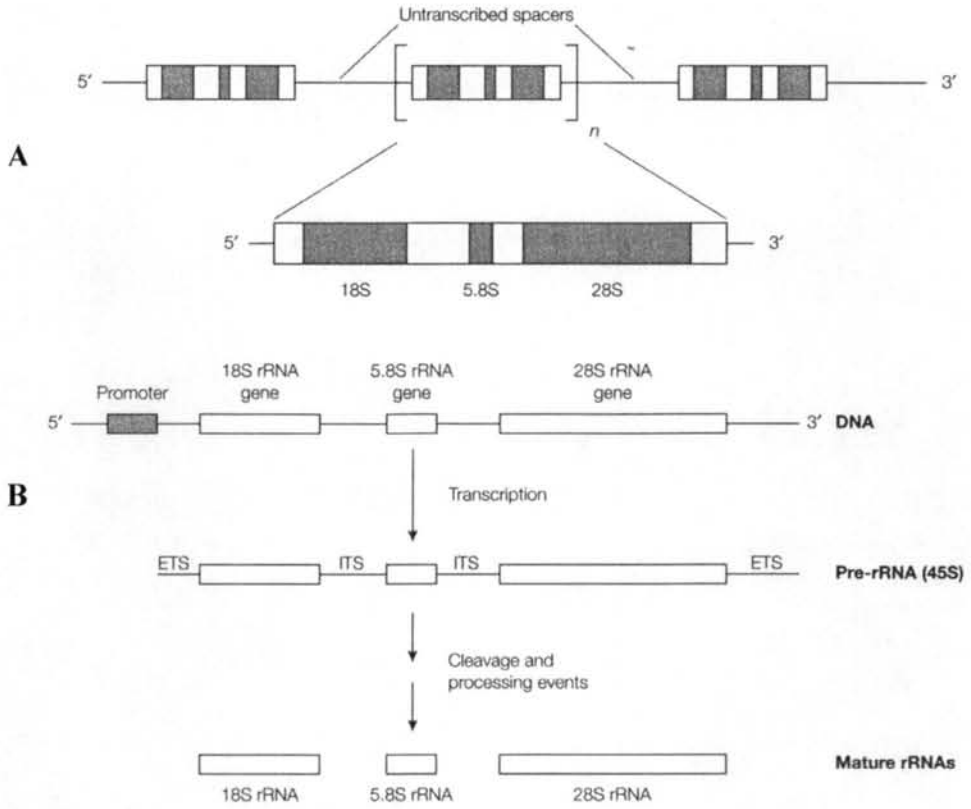

Figure 3. rDNA and pre-rRNA processing

(A) Organization of eukaryotic rDNA. Coding regions are shown as solid bars. (B) Transcription and processing of eukaryotic rDNA. The transcribed spacers are distinguished as external transcribed spacer (ETS) and internal transcribed spacer (ITS). RDNA are transcribed as a single 45S pre-rRNA. The ETSs and ITSs are removed by processing to form mature 18S, 5.8S and 28S rRNAs.

promoter core factor (CF) and TATA-binding protein (TBP) in yeast, and upstream-binding factor (UBF) and transcription initiation factor IB (TIF-IB) in mouse. PICs recruit an initiation-competent subfraction of Pol I, defined by the presence of RRN3/transcription initiation factor IA (TIF-IA) (Fig. 4) (Bodem et al., 2000; Miller et al., 2001).

Chapter 3: nucleolus

Nucleoli form around clusters of rDNA repeats at the nucleolar organizer regions (NORs) on one or more chromosomes. The nucleolus is the site of rRNA production and contains hundreds of tandem rDNA and a large number of factors involved in transcription, processing and the assembly of rRNA. The main body of the nucleolus of metabolically active cells is made up of particles 15-20 nm in diameter and hence termed granular component (GC). Embedded in this granular mass are one or several islets of rounded structures of relatively low contrast, the fibrillar centers (FC). These are invariably surrounded, either wholly or in part, by a layer consisting of tightly packed and densely staining fibrils, the dense fibrillar component (DFC) (Ulrich Scheer, 1990). rDNA transcription takes place at the boundary between the fibrillar center and the dense fibrillar component (Hozak et al., 1994). Also, transcription of the rDNA maintains the normal structure of nucleolus (Nomura, 2001; Ulrich Scheer, 1990).

In addition to the production of rRNA, the nucleolus has many other important functions, such as cell-cycle regulation and control of senescence, stress responses and nuclear export pathways (Mayer and Grummt, 2005; Olson, 2004; Olson et al., 2002). Recent studies suggest that some of these functions are achieved by nucleolar confinement, in which molecules participating in reaction chains are separated from their target molecules. Since the existence of the nucleolus depends on the ongoing synthesis of rRNA, the regulation of Pol I activity is crucial for the physiology of the cell.

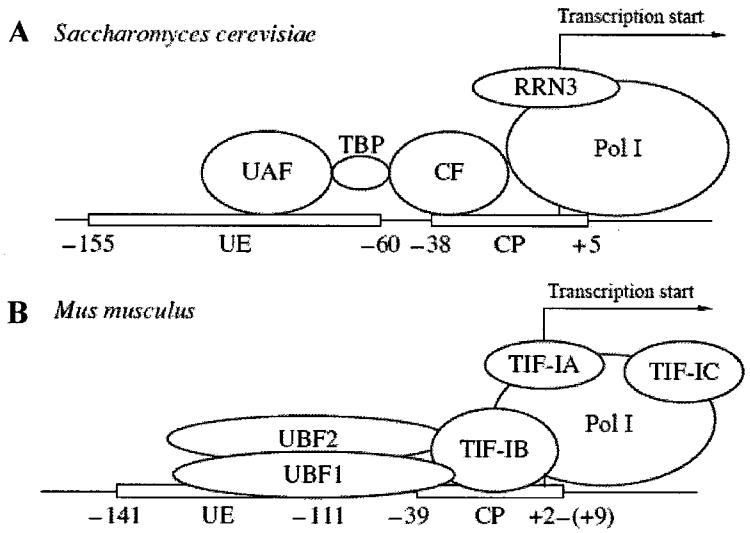

Figure 4. RNA polymerase I promoter and transcription factors

Modes of transcription initiation complexes formed on rDNA promoters in yeast (A) and in mouse (B). RNA polymerase I promoter consists of core promoter (CP) and upstream element (UE). Pre-initiation complexes (PICs) includes upstream activating factor (UAF) and promoter core factor (CF) and TATA-binding protein (TBP) in yeast, and upstream-binding factor (UBF) and transcription initiation factor IB (TIF-IB) in mouse. PICs recruit an initiation-competent subfraction of Pol I, defined by the presence of RRN3 in yeast and transcription initiation factor IA (TIF-IA) in mouse.

Chapter 4: RNA polymerase I and the second largest subunit

Eukaryotes have three structurally similar RNA polymerases, which are huge multi-subunit protein complexes. Pol I transcribes the rDNA. RNA polymerase II (Pol II) transcribes protein-encoding genes into messenger RNA (mRNA). Pol III transcribes the 5S rDNA and all the transfer RNA (tRNA) genes. The two largest polypeptides in the three RNA polymerases, which represent two-thirds of the mass of the enzyme molecule, are homologous to β and β'subunits of the *Escherichia coli* enzyme (Sweetser et al., 1987) and form the polymerase active center (Fig. 5) (Cramer et al., 2001). SDS-PAGE analysis of mammalian Pol I revealed that Pol I consists of 14 peptide with the molecular masses of 180, 114, 53, 51, 49, 44, 40, 27, 20, 18, 16, 15, 14, and 12 kDa (Song et al., 1994). Among them, 9 subunits are conserved in metazoa, including humans, and called 'core' subunits (Geiduschek and Bartlett, 2000; Song et al., 1994).

Rpo1-2 is the second largest subunit and is comprised of 15 exons and encodes 1135 amino acids (aa) (Seither and Grummt, 1996). Sequence alignment of the *Rpo1-2* subunit from mouse with *D. melanogaster* and *S. cerevisiae* RPA2 subunits revealed an overall homology of 49.3% and 49.6%, respectively. This sequence homology is significantly lower than that observed between the second largest subunits of Pol II and Pol III from *D. melanogaster* and yeast (74.8 and 72.9%) (Seither and Grummt, 1996). Rpo1-2 contains ten conserved domains (A-J) (Fig. 6)(Shematorova and Shpakovski, 2002; Sweetser et al., 1987), which occur only in components of multiple protein RNA polymerases. The C-terminal domain possesses a zinc-binding motif with consensus $Cx_2Cx_{24}Cx_2C$ (Shematorova and Shpakovski, 2002). Despite the low sequence homology of Rpo1-2 among the three species examined, general functions are expected to be executed by conserved regions.

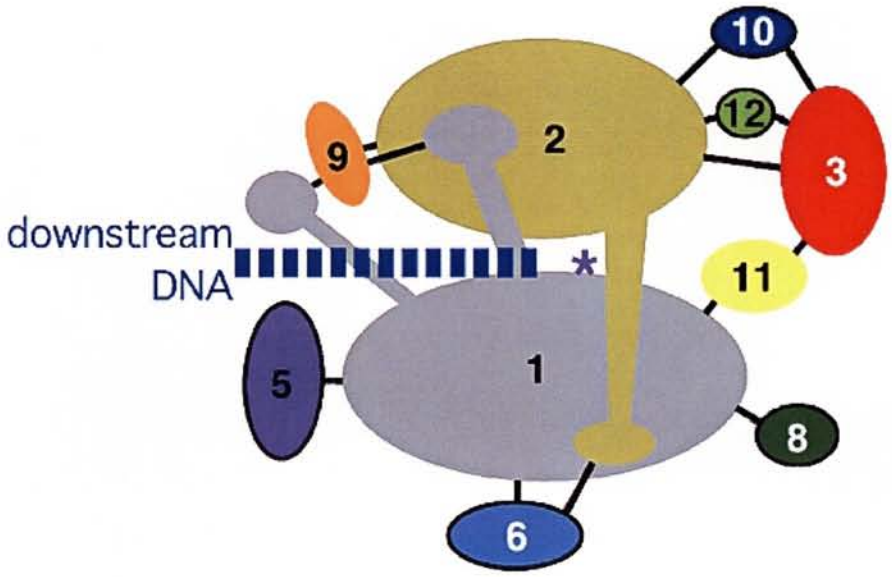

Figure 5. Architecture of RNA polymerases.

A network of contacts between Pol II subunits. Number indicates corresponding subunit. This is the model of the 10-subunit RNA polymerase II core. The purple asterisk symbolizes the catalytic center. The assembly of 1-2-3-5-6-8-10-11-12 nine-subunit can be regarded as the core of the three nuclear RNA polymerases.

(From Geiduschek and Bartlett, 2000)

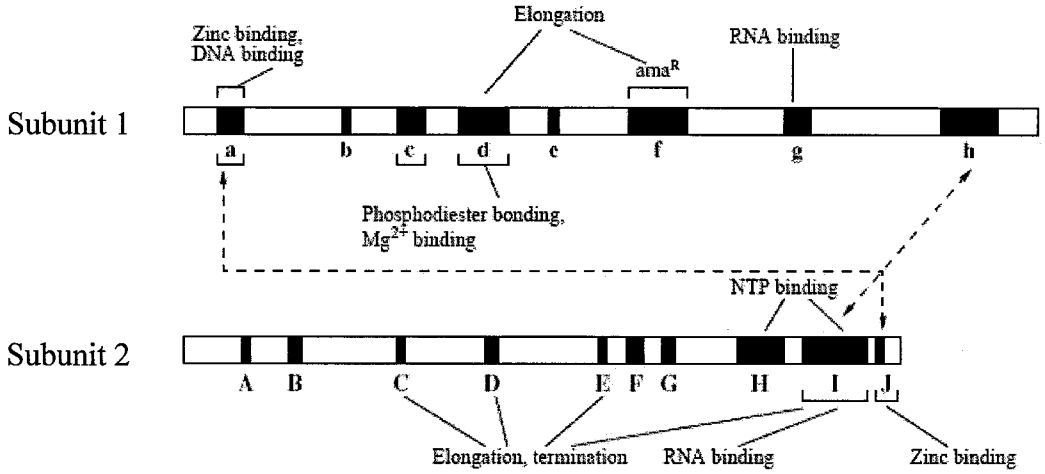

Figure 6. Structural and functional domains of the two largest subunits of eukaryotic Pol I.

Arrows link domains that interact on biochemical and genetic evidence. Black blocks indicate conserved domains.

(From Shematorova EK, Shpakovski GV., 2002.)

We have analyzed a strain of *Rpo1-2* mutant (*Rpo1-2*^{Gt}) mice generated by a gene trapping approach. Heterozygous mice displayed no obvious phenotype. In contrast, homozygous mutant embryos could develop to the morula stage, but thereafter they displayed nucleolar disruption and apoptosis, which resulted in death.

Materials and Methods

Establishment of gene trap clones and mouse lines

The gene trap vector pU-hachi and the isolation of gene trap clones have been previously described (Araki et al., 1999a). The ES cell line, TT2 (Yagi et al., 1993), was grown as described (Niwa et al., 1993) except for the use of G418-resistant primary mouse embryo fibroblasts as feeder layers.

In the case of electroporation with the pU-Hachi gene trap vector, 100 μg *Spe*I-digested DNA and 3×10^7 cells were used. The cells were suspended in 0.8 ml of PBS and then electroporated using a Bio-Rad Gene Pulser set at 800 V and 3 μF, and after 48 hours they were fed with medium supplemented with 200 μg/ml G418. Selection was maintained for 7 days, and then colonies were picked into 24-well plates and expanded for freezing. The trap clones were analyzed by Southern blotting to select cell lines showing a single-copy integration pattern.

Chimeric mice were produced by ES cells aggregation with eight-cell embryos of ICR mice (Nippon Clea, Tokyo, Japan), as previously described (Shimada et al., 1999). Chimeric male mice and their heterozygous progeny were backcrossed for four to six generations onto a C57BL/6J background.

Molecular cloning of gene trap flanking genomic regions by plasmid rescue

Plasmid rescue was performed as previously described (Fig. 1E) (Araki et al., 1999a). Genomic DNA (20 μg) of Ayu8019 ES cells was digested with *Xba*I or *Sph*I, followed by self-ligation in a reaction volume of 400 μl to obtain circular molecules. After phenol/chloroform extraction and ethanol precipitation, the DNA was suspended in 10 μl of TE and, using half of the DNA solution, *Escherichia coli* STBL2 (Life Technologies,

Maryland USA) was transformed through electroporation using a Bio-Rad Gene Pulser according to the manufacturer's recommendations. The electroporated cells were incubated in 1 ml of Circle Grow medium (BIO 101, Inc. Vista CA, USA) at 30°C for 1 hr. with shaking, and then concentrated and plated on LB/agar plates using ampicillin drug selection for the plasmids. The recovered plasmids were mapped using restriction enzymes and sequenced using the BigDye Terminator Cycle Sequencing (Perkin-Elmer, Foster City, CA).

Southern hybridization

Southern hybridization was done to confirm single-copy insertion of the vector. Mouse tail was digested with SDS/proteinase K, treated with phenol/chloroform, 1:1 (vol:vol) twice, precipitated with ethanol, and then dissolved in 10 mM Tris-HCl, pH 7.5/1 mM EDTA (TE). Ten micrograms of genomic DNA was digested with *Pst*I, *Bgl*II, *EcoR*I, *Sac*I, and *HinC*II, electrophoresed on a 0.9% agarose gel and then blotted onto a nylon membrane (Roche Applied Science, Penzberg, Germany). Hybridization was performed using a DIG DNA Labeling and Detection Kit (Roche).

Collection of preimplantation embryos

Eight to twelve week female mice were superovulated by intraperitoneal injection of 5 IU of pregnant mare serum gonadotropin (PMS), followed 44-50 h later by 5 IU of human chorionic gonadotropin (hCG). They were mated with male mice, and 2-cell or 8-cell stage embryos were collected and cultured in KSOM (Erbach et al., 1994) medium at 37°C.

Genotyping of mice and preimplantation embryos

Mouse genomic tail DNA was prepared according to standard procedures. The wild-type *Rpo1-2* allele was detected with primers S1 (5'-TCAGAGAAGTTTAAGCAGGGAG-3') and AS1 (5'- GGGCATCACTCATTATATCAGG-3'). Primers Z8 (5'-GTTTTACAACGTCGTG

ACTGG-3') and Z2 (5'-TGTGAGCGAGTAACAACC-3') were used to identify the *Rpo1-2*^{Gt} allele. PCR conditions were 30 cycles of 94°C for 30 sec, 60°C for 30 sec, and 72°C for 60 sec.

For 2-cell to blastocyst stage embryos, individual embryos were lysed for 5 min in 2μl of 0.005% SDS, 0.035 N NaOH at 100°C. After dilution with 36μl of water, PCR was carried out using 5μl of the extract. For fixed preimplantation stage embryos, individual embryos were lysed for 15 min in 3μl of 0.1N NaOH at 100°C. After neutralization with 9μl 0.1M Tris-HCl (pH 8.0), PCR was carried out using 3μl of the extract. The wild-type allele was detected with primer S1 and AS1 followed by nested primers S2 (5'-CAGAAGCTGGAC GATGATGG-3') and AS2 (5'-CTGACCAATCAGGTTCCCAG-3'). The mutant allele was detected with primer Z8 and Z2 followed by nested primers Z1 (5'-GCGTTACCCAACTTAA TCG-3') and LZUS3 (5'- CGCATCGTAACCGTGCATC-3'). PCR conditions were 30 cycles of 94°C for 30 sec, 60°C for 30 sec, and 72°C for 60 sec.

RNA isolation and Northern blot analysis

Total RNA was extracted with Sepasol RNA I (Nacalai Tesque, Kyoto, Japan) according to manufacture's instructions. Ten μg of total RNA per lane was electrophoresed on 1% agarose-formaldehyde gels, transferred to Nylon membranes (Roche Applied Science, Penzberg, Germany), and hybridized with probes prepared using a DIG RNA Labeling and Detection Kit (Roche).

To compare the mature rRNA level between wild and *Rpo1-2*$^{Gt/+}$ mice, total RNA was isolated from same amount tissue. One-sixth and one-thirtieth of total RNA per lane was electrophoresed on 1% agarose-formaldehyde gels separately.

Embryonic expression pattern of *Rpo1-2*^{Gt}

At 9.5 days post coitus (dpc), embryos dissected from heterozygous intercrosses were fixed for 30 to 60 minutes at 4°C in 1% paraformaldehyde, 0.2% glutaraldehyde, and 0.02% Nonidet P-40 (NP-40)/PBS. Fixed embryos were washed twice in PBS and incubated overnight at 30°C in X-gal staining solution: 5mM potassium ferricyanide, 5mM potassium ferrocyanide, 2mM $MgCl_2$, and 0.1% X-gal in PBS.

Preimplantation embryos were fixed in 1% glutaraldehyde for 5 minutes, and permeabilized in 1% Triton X-100 for 5 minutes, then embryos were incubated over night at room temperature in staining solution.

RT-PCR analysis with preimplantation embryos

Total RNA was isolated from individual preimplantation embryos using the RNeasy Mini Kit (QIAGEN, Valencia, CA) and resuspended in 30 µl DW. First-strand cDNA was synthesized using 9 µl RNA solution with random hexamer primers according to the ThermoScript RT-PCR system (Invitrogen, Carlsbad, CA). A one-tenth volume of the first-strand reaction was use for PCR amplification.

Primers pre-rRNA forward (5'-GAGAGTCCCGAGTACTTCAC-3') and pre-rRNA reverse (5'-GGAGAAACAAGCGAGATAGG-3') in the 5' external transcribed spacer (5'-ETS) region of 45S pre-rRNA (Strezoska et al. 2000) were used. 18S rRNA was detected by primers 1+ (5'-AGCCTGAGAAACGGCTACCACATC-3') and 1– (5'-AGACTT GCCCTCCAATGGATCCTC-3'). Rpo1-2 mRNA was detected by nested PCR using, in the 1st round, primers RpoS2 (5'-AAACTCTATCGACTCCAAACCC-3') in exon 13 and RpoAS1 (5'-TCATGCCACTCTCAGTGAAAGG-3') in exon 15 and, in the 2nd round, primers RpoS3 (5'-ATAACCTGGTGTTCGGGGTCAA-3') in exon 14 and RpoAS2 (5'-GCC ACAATCTGCTCAAAATGC -3') in exon 15. The fusion transcript of *Rpo1-2* and *βgeo* was

detected by nested PCR with 1st round primers RpoS2 and loxP-B (5'-GATCCGGAACCCTT AATATAAC-3') and 2nd round primers RpoS3 and lox71-PR (5'-CGGTATAGGTCCCTCG ACC-3'). Conditions for all the reactions were: 30 cycles of 94°C for 30 sec, 60°C for 30 sec, and 72°C for 60 sec.

Immunohistochemical analysis with preimplantation embryos

Apoptosis was determined by terminal deoxynucleotidyl transferase (TdT) mediated dUTP nick end labeling (TUNEL) staining, using In Situ Cell Death Detection kit (Roche, Penzberg, Germany). Briefly, embryos were fixed in 4% paraformaldehyde-PBS for 1 h, and permeabilized in 0.5% Triton X-100 for 30 minutes, then embryos were incubated with TdT and fluorescein-labeled dUTP reaction mixture at 37°C for 1 h. Then, for B23/nucleophosmin (NPM) immunohistochemistry, embryos were incubated overnight at 4°C with monoclonal mouse anti-B23 antibody (Zymed, Clone Fc-61991; dilution 1:100). After blocking with 5% normal goat serum, embryos were then incubated with fluorescence labeled goat anti-mouse IgG (dilution 1:200, Invitrogen detection technologies). The nuclei were counterstained with DAPI. Samples were examined using a Leica TCS SP2/ DM-IREM2 inverted confocal microscope (Leica Microsystems Inc).

Results

Characterization of the gene trap event in clone Ayu8019 and generation of an *Rpo1-2* mutant line

Clone Ayu8019 was isolated by gene trap screening with the pU-Hachi trap vector (Fig.7A) and single integration was confirmed by Southern blot (Araki et al., 1999a). Genomic DNA flanking the integration site was obtained by plasmid rescue (Araki et al., 1997; Araki et al., 1999a), and GenBank database searches revealed that the trap vector had integrated into the exon 14 of *Rpo1-2* (Fig. 7B). No gross deletion or rearrangement was found at the integration site. Integration pattern was confirmed by Southern blot with a probe for the pUC vector fragment (Fig. 8). Since the trap vector had integrated into an exon, we analyzed the fusion transcript created between *Rpo1-2* and *βgeo*, of the trap vector, by RT-PCR using primers in exon 13 and in *βgeo*. Sequence analysis revealed that the fusion transcript spliced between a cryptic splice-donor site (position 65 in the pU-hachi sequence, GenBank accession No. AB242616) in *En-2* intron sequence and the authentic splice acceptor site of *En-2*, a component of the trap vector (Fig. 7D). This predicted a fusion protein containing 824 aa of the N-terminal of Rpo1-2 and 101 aa derived from trap vector sequence (Fig. 7C).

Chimeric mice were produced by aggregation of Ayu8019 ES cells with ICR morulae and the mutant allele was transmitted through the germ line. The established line was designated as B6.CB-*Rpo1-2*$^{GtpU\text{-}HachiIMEG}$ (*Rpo1-2*^{Gt}).

Analysis of *Rpo1-2*^{Gt} expression in *Rpo1-2*$^{Gt/+}$ mice

To confirm expression levels of *Rpo1-2*^{Gt}, we performed Northern blot analysis with a 5'-probe, which detects both endogenous and fusion transcripts, a 3'-probe which detects only

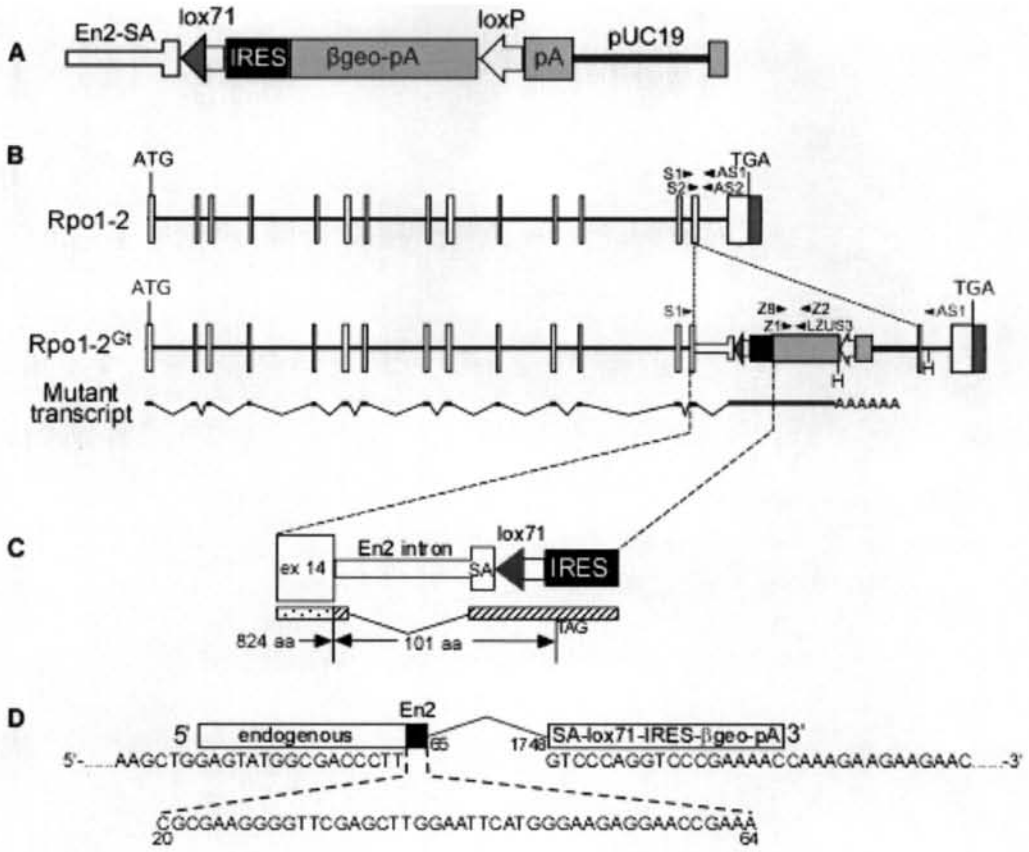

Figure 7. gene trap events in the Ayu8019 line.

(A) Structure of the trap vector, pU-hachi. The pU-hachi vector contains a splice acceptor region (SA) from mouse En-2, lox71, the internal ribosomal entry site (IRES) from the encephalomyocarditis virus (ECMV), the β-galactosidase/neomycin phosphotransferase fusion gene (βgeo), loxP, the SV40 polyadenylation sequence (pA), and pUC19. (B) Integration and transcription pattern of the trap vector. pU-hachi vector was inserted 202bp downstream on exon 14. Arrow-heads indicate primers used for genotyping. H, HincII. (C) Fusion protein of trapped allele. The fusion protein is predicted to contain 824aa of the N-terminal portion of Rpo1-2 protein and 101aa derived from the trap vector. (D) Junction sequence of fusion transcript. The fusion transcript was spliced between a cryptic splice-donor site in the intron sequence (position 65 in the pU-hachi sequence) and the SA of the En-2 gene

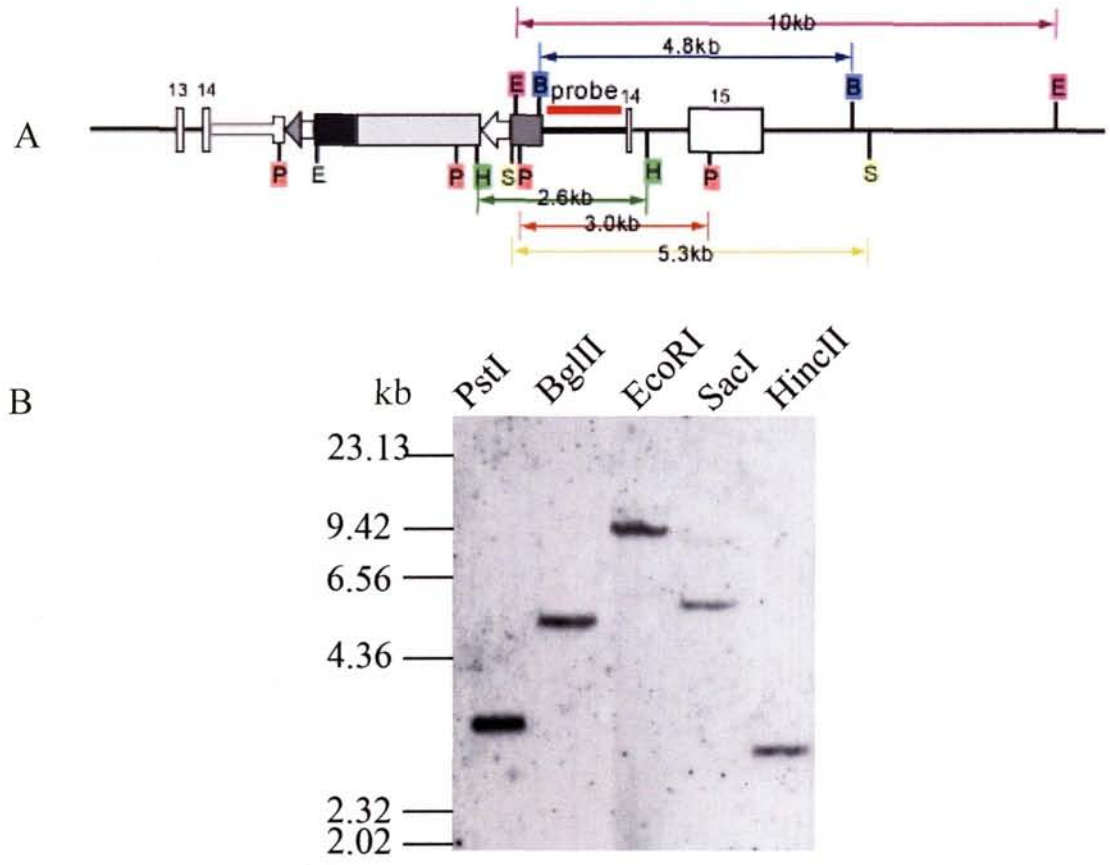

Figure 8. Trap vector integration pattern was confirmed by Southern blot.

(A) Integration pattern of the pU-Hachi vector in Rpo1-2 and the expected fragment using different restriction enzyme. P, PstI. H, HinCII. S, SacI. E, EcoRI. B, BglII. (B) Southern blot analysis of Rpo1-$2^{Gt/+}$ mice genomic DNA using probe shown in (A).

the endogenous transcript and with a *LacZ* probe which detects only the fusion transcript (Fig. 9A). Wild type expressed a 4 kb endogenous *Rpo1-2* transcript in all tissues examined, as expected from the fact that The *Rpo1-2* is a housekeeping gene. *Rpo1-2*$^{Gt/+}$ mice expressed a 7.5 kb fusion transcript, which was also detected with the LacZ probe, as well as the endogenous transcript (Fig. 9B). In *Rpo1-2*$^{Gt/+}$ mice, the expression level of the endogenous transcript was almost half that of wild type and, interestingly, the expression level of the fusion transcript was stronger than that of the endogenous transcript (Fig. 9B).

Next we analyzed *Rpo1-2*^{Gt} expression pattern by measuring β-galactosidase activity. Whole-mount X-gal staining of 9.5 dpc *Rpo1-2*$^{Gt/+}$ embryos showed ubiquitous, but strong expression of *Rpo1-2*^{Gt} in highly proliferating tissues (Fig. 10). The fact that the βgeo protein was translated from the *Rpo1-2*^{Gt} fusion mRNA suggests that the truncated Rpo1-2 protein can be translated in *Rpo1-2*$^{Gt/+}$ mouse.

Mature rRNA level in wild and *Rpo1-2*$^{Gt/+}$ embryos

Rpo1-2$^{Gt/+}$ heterozygous mice were healthy, fertile, and appeared normal. Since no obvious phenotype was observed in *Rpo1-2*$^{Gt/+}$ mice, we tried to detect the rRNA synthesis in *Rpo1-2*$^{Gt/+}$ mice. We compared the 18S and 28S rRNA level between wild and *Rpo1-2*$^{Gt/+}$ mice. Total RNA was isolated from same weight of kidney tissue from 5-day-old mice, 3 mice for each genotype. One-sixth and one-thirtieth of total RNA was electrophoresed on a 1% agarose-formaldehyde gel and compared the intensity of the 18S and 28S bands. No obvious difference was found between wild and *Rpo1-2*$^{Gt/+}$ mice (Fig. 11). Although the *Rpo1-2* mRNA level in *Rpo1-2*$^{Gt/+}$ mice is almost half of wild mice, the rDNA transcription activity in *Rpo1-2*$^{Gt/+}$ mouse was not affected at all.

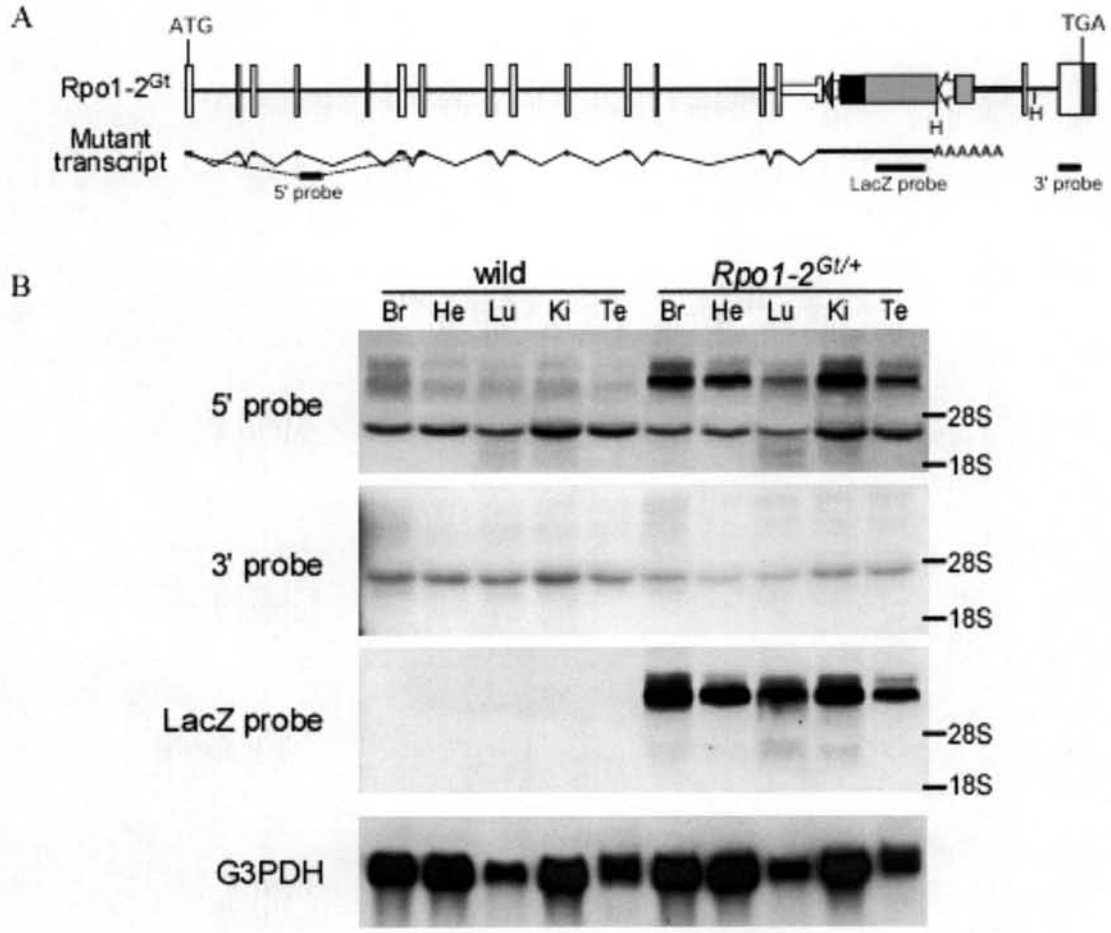

Figure 9. Expression levels of Rpo1-2^{Gt} was confirmed by Northern blot.

(A) The solid bars show the probe used in northern blotting. 5'-probe detects both endogenous and fusion transcripts, 3'-probe detects only the endogenous transcript and *LacZ* probe detects only the fusion transcript. (B) Northern analysis of wild type and Rpo1-2$^{Gt/+}$ mice. Wild type mouse expressed a 4 kb endogenous *Rpo1-2* transcript in all tissues examined *Rpo1-2*$^{Gt/+}$ mice expressed a 7.5 kb fusion transcript, as well as the endogenous transcript. In *Rpo1-2*$^{Gt/+}$ mice, the expression level of the endogenous transcript was almost half that of wild type and the expression level of the fusion transcript was stronger than that of the endogenous transcript. Br, brain; He, heart; Lu, lung; Ki, kidney; Te, testis.

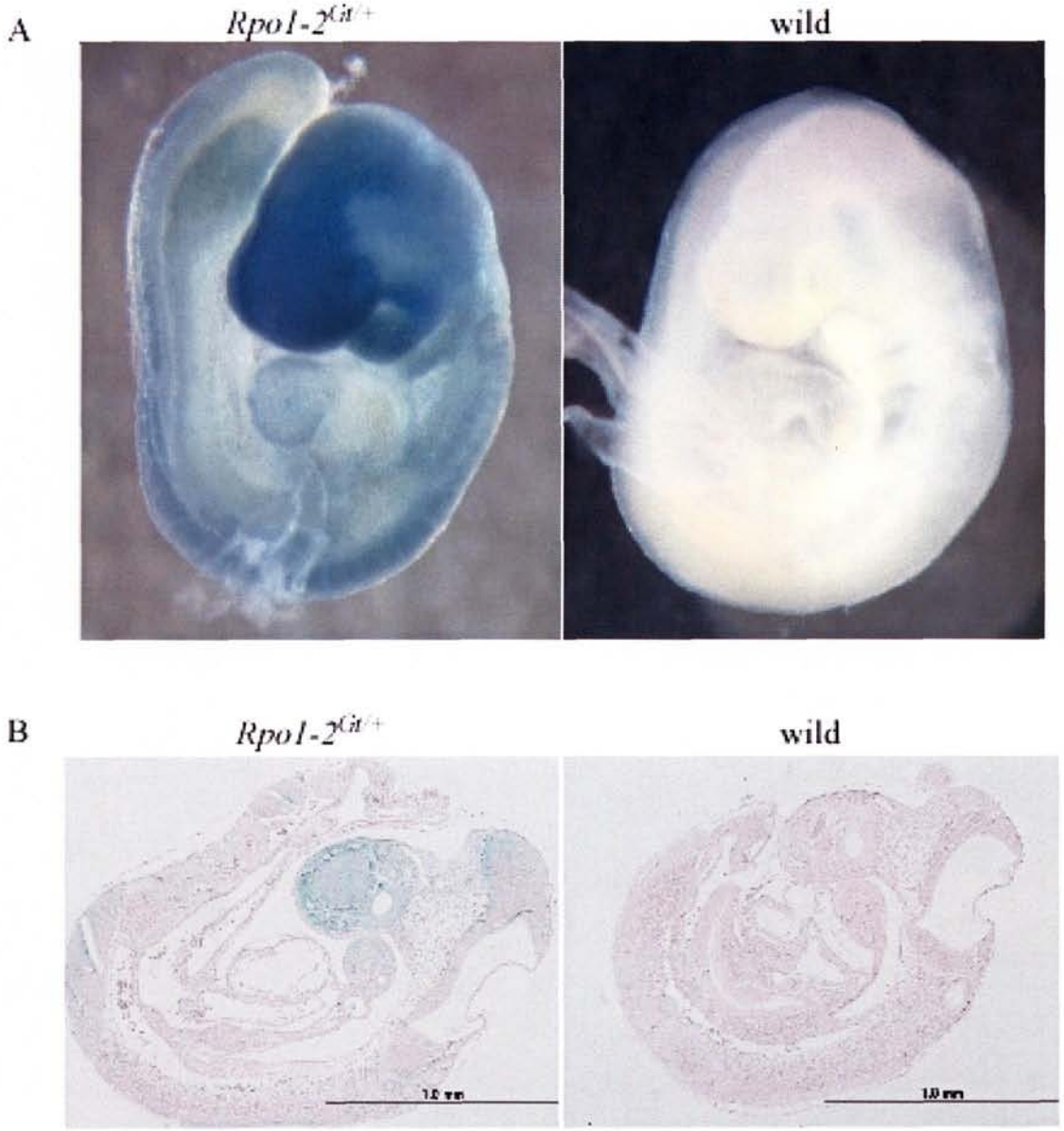

Figure 10. Analysis of Rpo1-2^{Gt} expression in 9.5 dpc Rpo1-2$^{Gt/+}$ embryos.

(A) Whole-mount X-gal stain of 9.5 dpc embryos. (B) Fast red-stained wax section of embryos in (A).

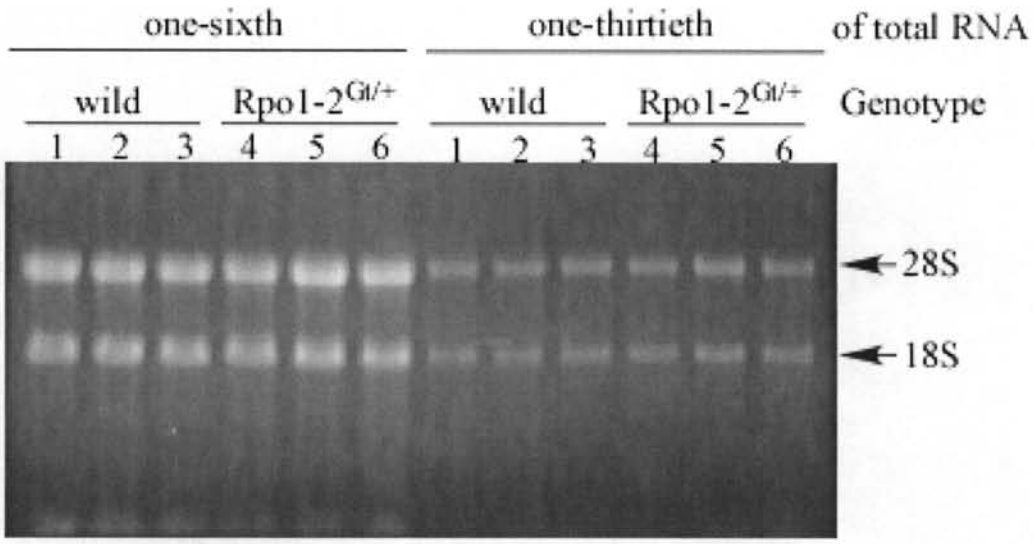

Figure 11. Mature rRNA level comparison between wild and Rpo1-2$^{Gt/+}$ mouse

Total RNA was extracted from same amount kidney tissue of 5-day-old mice, 3 mice for each genotype. One-sixth or one-thirtieth per lane of total RNA was electrophoresed on one gel. No obvious difference was found between wild and Rpo1-2$^{Gt/+}$ mice.

Rpo1-2$^{Gt/Gt}$ homozygous embryos died at the morula stage

To examine the phenotype of *Rpo1-2*$^{Gt/Gt}$ homozygous mice, *Rpo1-2*$^{Gt/+}$ mice were intercrossed and their progeny genotyped. Of 32 newborn mice, 34% were *Rpo1-2*$^{+/+}$, and 66% were *Rpo1-2*$^{Gt/+}$, indicating that homozygous mice were embryonic lethal (Table1). From embryos isolated between 7.5dpc and 9.5dpc, no *Rpo1-2*$^{Gt/Gt}$ embryos were identified (Table1). Also, we did not observe any empty deciduas, suggesting that *Rpo1-2*$^{Gt/Gt}$ embryos failed to implant onto the uterine wall.

To examine how the *Rpo1-2*^{Gt} mutation affects early embryogenesis, we collected embryos from heterozygous intercrosses at the 2-cell stage, observed their growth in culture until the blastocyst stage (Fig. 12), and genotyped embryos at each stage by PCR (Table 2). Wild type and *Rpo1-2*$^{Gt/+}$ embryos differentiated to cavitating blastocysts and finally expanded to form an inner cell mass (ICM) and the outer trophoblast cell layer (Fig. 13). *Rpo1-2*$^{Gt/Gt}$ embryos were initially indistinguishable from wild type and *Rpo1-2*$^{Gt/+}$ embryos until the morula stage (Fig. 12), and the expected Mendelian frequency of *Rpo1-2*$^{+/+}$, *Rpo1-2*$^{Gt/+}$and *Rpo1-2*$^{Gt/Gt}$ morulae was observed (Table 2). However, all *Rpo1-2*$^{Gt/Gt}$ embryos failed to form a normal blastocoel and ICM, and became progressively more disorganized and fragmented with extensive cellular degeneration (Table 2, Fig. 13). This indicates that the *Rpo1-2*^{Gt} allele induced embryonic lethality at the late morula stage.

Rpo1-2^{Gt} expression in pre-implantation embryos

In order to reveal when the expression of *Rpo1-2* and *βgeo* fusion mRNA start, we performed X-gal staining with pre-implantation embryos obtained from heterozygous intercrosses. At 2-cell stage, no embryos were X-gal positive (Fig. 14A). At 64 hphCG, most embryos are 4-cell stage and β-galactosidase activity can be detected in 65% of embryos (11 embryos were

Table 1. Distribution of genotyped offspring and embryos from *Rpo1-2*$^{Gt/+}$ intercrosses

Genotype	New born	9.5 dpc	8.5 dpc	7.5 dpc
+/+	11	3	9	17
Gt/+	21	4	22	39
Gt/Gt	0	0	0	0
Unknown	0	0	1	1
Empty decidua	0	0	1	1
Total	32	7	33	58

Table 2. Genotype analysis of preimplantation embryos from *Rpo1-2*$^{Gt/+}$ intercrosses.

genotype	1.5 dpc	2.5 dpc	3.5 dpc		
	2-cell	morula	blastocyst	degenerated	Total
+/+	3	7	21	1	22
+/Gt	2	21	33	4	37
Gt/Gt	4	5	0	11	11
Unknown	4	6	4	5	9
Total	13	39	58	21	79

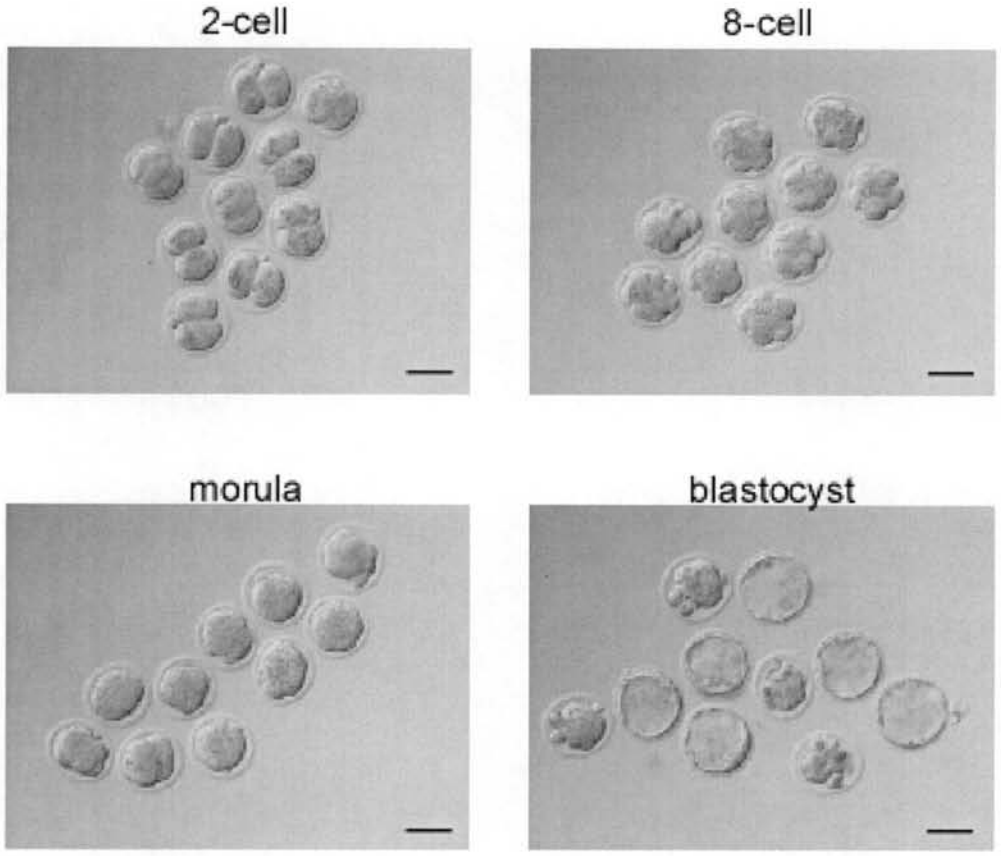

Figure 12. Development of *Rpo1-2*$^{Gt/Gt}$ embryos

Two-cell embryos were obtained from heterozygous intercrosses and kept in KSOM medium till blastocyst stage. The same 10 embryos were photographed at each indicated developmental stage. Scale bar = 50 μm.

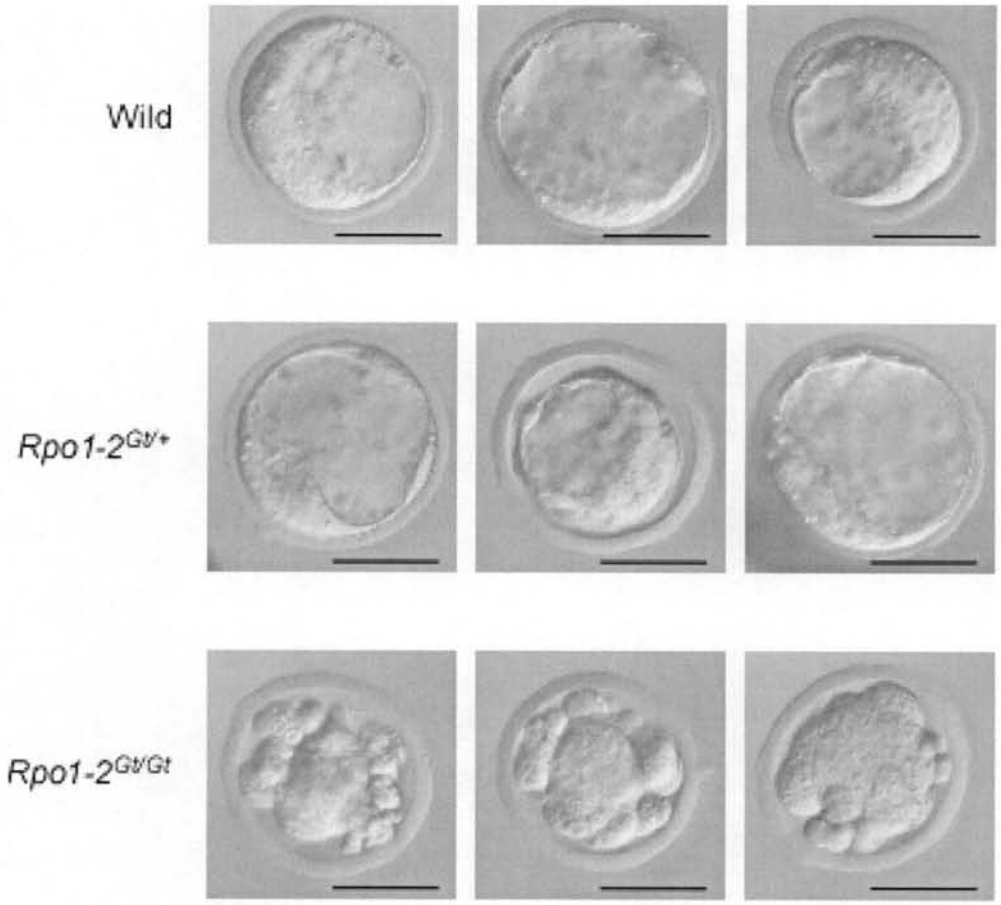

Figure 13. Phenotype of *Rpo1-2*$^{Gt/Gt}$ embryos

Phenotype of wild type, *Rpo1-2*$^{Gt/+}$ and *Rpo1-2*$^{Gt/Gt}$ embryos at blastocyst stage. All *Rpo1-2*$^{Gt/Gt}$ embryos were arrested at the morula stage, and exhibit signs of degeneration. Scale bar = 50 μm.

positive in total 17 embryos) (Fig. 14B). At 90 hphCG, 1 is degenerated morula, 7 embryos are blastocysts and 15 embryos are normal morulae. 70% (16/23) of embryos showed β-galactosidase activity, among them are 1 degenerated morula (4%), 3 normal blastocysts (13%), and 12 normal morulae (52%) (Fig. 14C). According to developmental results, X-gal stain positive normal blastocysts should be *Rpo1-2*$^{Gt/+}$, and the degenerated morula should be *Rpo1-2*$^{Gt/Gt}$. This result suggests the expression of the *Rpo1-2* gene become active from 4-cell stage embryo, in the both *Rpo1-2*$^{Gt/Gt}$ and *Rpo1-2*$^{Gt/+}$ embryos. Since no X-gal positive signal could be detected at 2-cell stage, it is considered that even maternal *Rpo1-2*^{Gt} allele is not active at this stage as far as examined by X-gal staining.

Pre-rRNA synthesis is severely impaired in *Rpo1-2*$^{Gt/Gt}$ embryos

To investigate whether the *Rpo1-2*^{Gt} allele results in a reduction of rRNA synthesis, we performed RT-PCR analyses to detect pre-rRNA and mature 18S rRNA in morulae and in blastocysts obtained from heterozygous intercrosses. Since it is difficult to prepare DNA for genotyping and RNA for RT-PCR from a single embryo at the same time, genotypes were determined by RT-PCR detecting wild-type *Rpo1-2* transcript and/or the fusion transcript from the *Rpo1-2*^{Gt} allele [Fig. 15A, (a), (b)]. Wild type and *Rpo1-2*$^{Gt/+}$ embryos produced the expected RT-PCR products, however, some embryos showed a band of an unexpected size (429bp) with primers detecting wild-type transcript (Fig 15B). Sequence analysis revealed that alternative splicing occurred between a cryptic splice-donor site (position 1864 in the pU-hachi) within the exon sequence of *En-2* and the splice acceptor of exon 15 of *Rpo1-2* [Fig. 15A (c)]. Therefore, embryos showing the 429-bp band with WT primers and a 321-bp band with *Rpo1-2*^{Gt} primers should be homozygous for the *Rpo1-2*^{Gt} allele. Since we did not detect such aberrant transcripts in heterozygous embryos, nor in adult tissues, we consider that this alternative splicing occurred rarely. The resulting ORF of the alternative transcript is in frame

(A) 2-cell stage

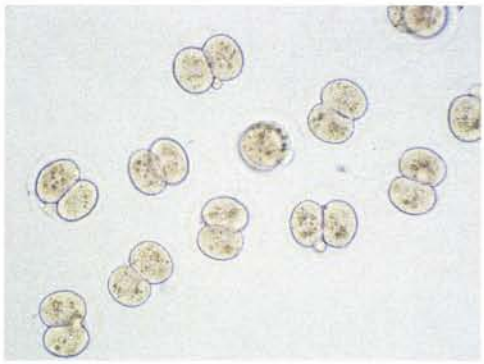

(B) 64 hphCG

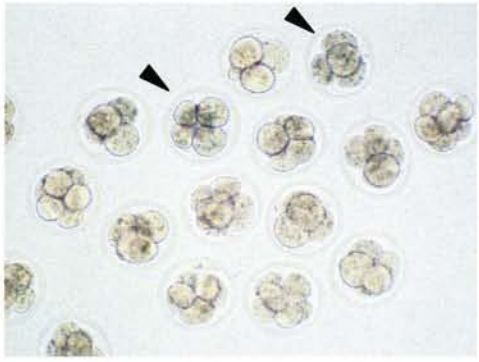

(C) 90 hphCG

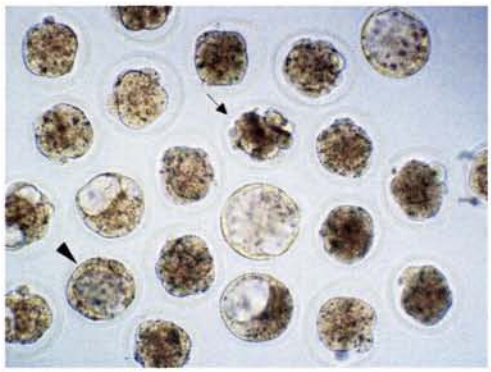

Figure 14. Analysis of Rpo1-2^{Gt} expression in preimplantation embryos.

X-gal stain of preimplantation embryos obtained from Rpo1-2$^{Gt/+}$ intercrosses. Three groups were stained at different stage. (A) No X-gal stain was found at 2-cell stage. (B) Arrow head indicates X-gal stain positive embryos. (C) Arrow indicates X-gal positive degenerated morula and arrow head indicate X-gal positive blastocyst.

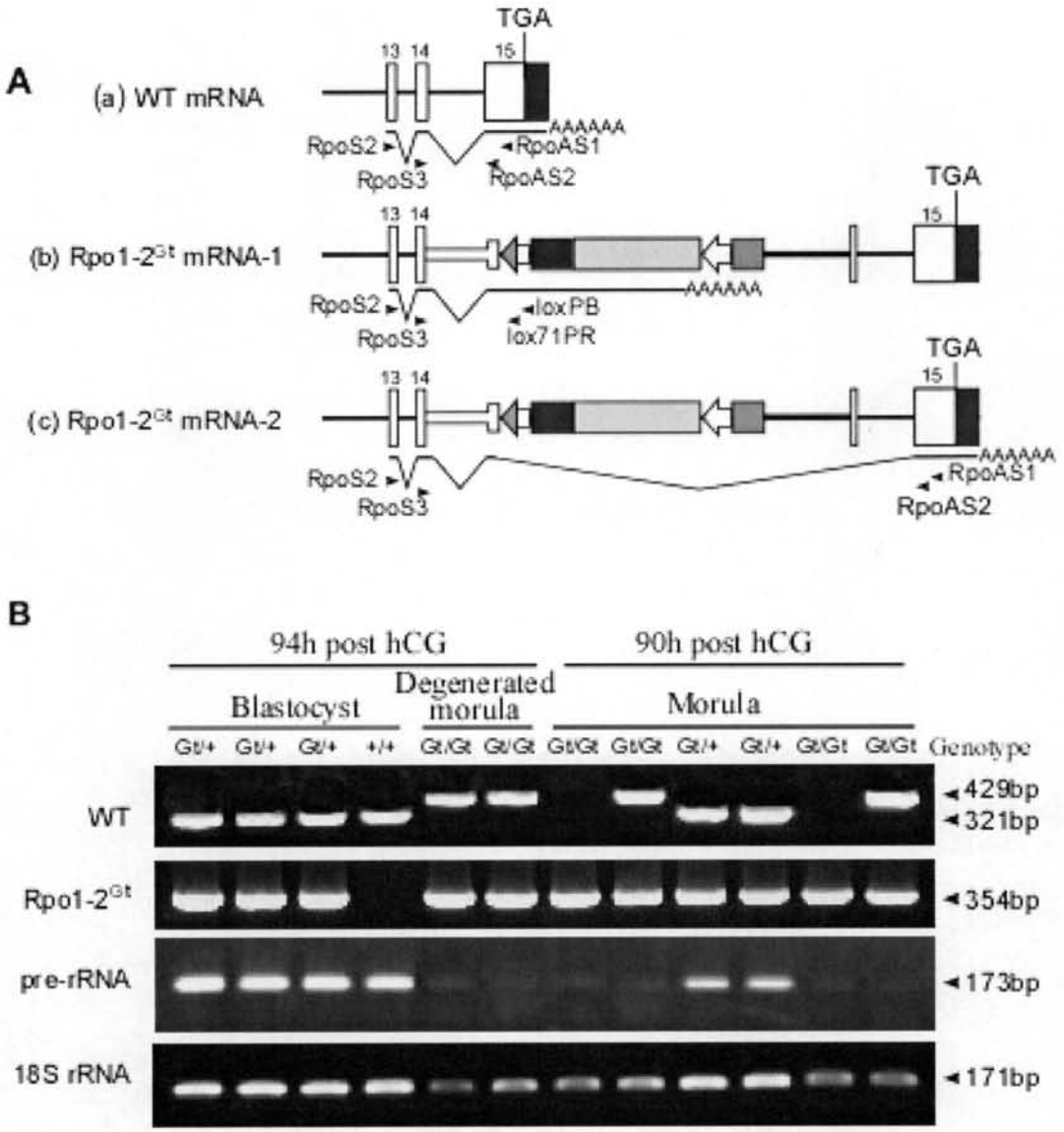

Figure 15. RT-PCR analyses of preimplantation embryos from Rpo1-2$^{Gt/+}$ intercrosses.

Transcription pattern of wild type (a) and Rpo1-2^{Gt} allele (b, c). (A) Primers used for RT-PCR genotyping are indicated with allow head. (B) Detection of pre-rRNA synthesis and 18S rRNA in embryos at 94h post hCG and at 90h post hCG. Genotypes determined from RT-PCR (shown in upper two photos) are indicated on the top of each lane.

with the endogenous ORF, and 18 aa of the C-terminal sequence of ex14 were replaced by 54 aa from the trap vector (Fig. 16). The phenotype of *Rpo1-2*$^{Gt/Gt}$ embryos expressing this alternative transcript was identical to the phenotype *Rpo1-2*$^{Gt/Gt}$ embryos that did not express the alternative transcription, indicating that the protein translated from the alternative transcript has the same defect as the mutant protein from the normal fusion transcript.

As shown in Fig. 15B, at the blastocyst stage (94h post-hCG), the synthesis of pre-rRNA was drastically reduced and the amount of 18S rRNA was also decreased in degenerated *Rpo1-2*$^{Gt/Gt}$ embryos. Interestingly, at the morula stage (90h post-hCG), when the morphology of *Rpo1-2*$^{Gt/Gt}$ embryos was normal, levels of both pre-rRNA and of 18S rRNA were already decreased. These results indicate that the function of the mutant Rpo1-2 protein is severely impaired and maternally inherited mature rRNAs are exhausted at the morula stage.

Nucleolar disruption and apoptosis in *Rpo1-2*$^{Gt/Gt}$ embryos

Transcription of rRNA is essential for maintaining nucleolar integrity (Nomura, 2001; Ulrich Scheer, 1990) and aberrant ribosome biogenesis causes nucleolar stress leading to p53-mediated apoptosis (Yuan et al., 2005). To examine whether the impaired pre-rRNA synthesis induces nucleolar/ nucleolar precursor bodies (NPBs) disruption in pre-implantation embryos we performed immuno-fluorescence staining with anti-B23/nucleophosmin (NPM) and to determine levels of apoptosis we performed the TUNEL assay. B23/NPM, which is often used as a marker of the nucleolus and of NPBs (Rubbi and Milner, 2003), regulates the stability and activity of p53 (Colombo et al., 2005) and alters localization from nucleolus to the nucleoplasm upon nucleolar disruption in response to several DNA binding agents (Chan et al., 1996).

Intercross embryos were collected at the 8-cell stage and cultured for 24hrs, and when some embryos appeared to be disorganized, the embryos were processed for immunofluorescence

Figure 16. Sequence alignment of mouse wild-type and trapped alternative Rpo1-2 proteins

Alignment of mouse wild-type and trapped Rpo1-2 protein was carried out by GENETYX. Trapped amino acid sequence is derived from alternative transcript detected by wild-type transcript primer (Rpo1-2^{Gt} mRNA-2 in Figure 16). Amino acid sequence from exon 14 and 15 was indicated. In the trapped alternative allele, 18aa of the C-terminal sequence of ex14 were replaced by 54aa from the trap vector.

staining, followed by genotyping. As shown in Fig. 17, wild type and *Rpo1-2*$^{Gt/+}$ embryos displayed bright nucleolar fluorescence signals with anti-B23/NPM. In contrast, *Rpo1-2*$^{Gt/Gt}$ embryos, which were morphologically abnormal, exhibited weak and diffuse signals in the nucleoplasm, demonstrating that the nucleoli were disintegrated. TUNEL staining in *Rpo1-2*$^{Gt/Gt}$ embryos revealed a high number of intensely labeled cells, which is diagnostic of apoptotic cell death (Fig. 17), whereas, heterozygous and wild-type blastocysts showed very few apoptotic cells.

We then investigated whether the translocation of B23/NPM was observed in *Rpo1-2*$^{Gt/Gt}$ morulae, in which pre-rRNA synthesis was already decreased but with the apparent normal morphology. We obtained 50 2-cell embryos from heterozygous intercrosses that were then incubated in culture medium. Twenty-four hr later they were fixed and stained with anti-B23/NPM for nucleolus detection. Cell-number counting, with the aid of DAPI staining, showed that 5 embryos had 10-12 cells but all the others had only 8 cells, demonstrating they were at the early morula stage. Among 50 morulae, 38 (76%) embryos had intact and intense nucleoli staining, and the other 12 (24%) embryos showed weak and broad signals, indicating nucleolar disruption (Fig. 18). Although we failed to genotype these fixed and stained morulae, we consider the 24% embryos showing B23/NPM translocation as *Rpo1-2*$^{Gt/Gt}$ embryos, based on Mendelian frequency. These results suggest that impaired pre-rRNA transcription led to nucleolar disruption, followed by apoptotic cell death in pre-implantation embryos.

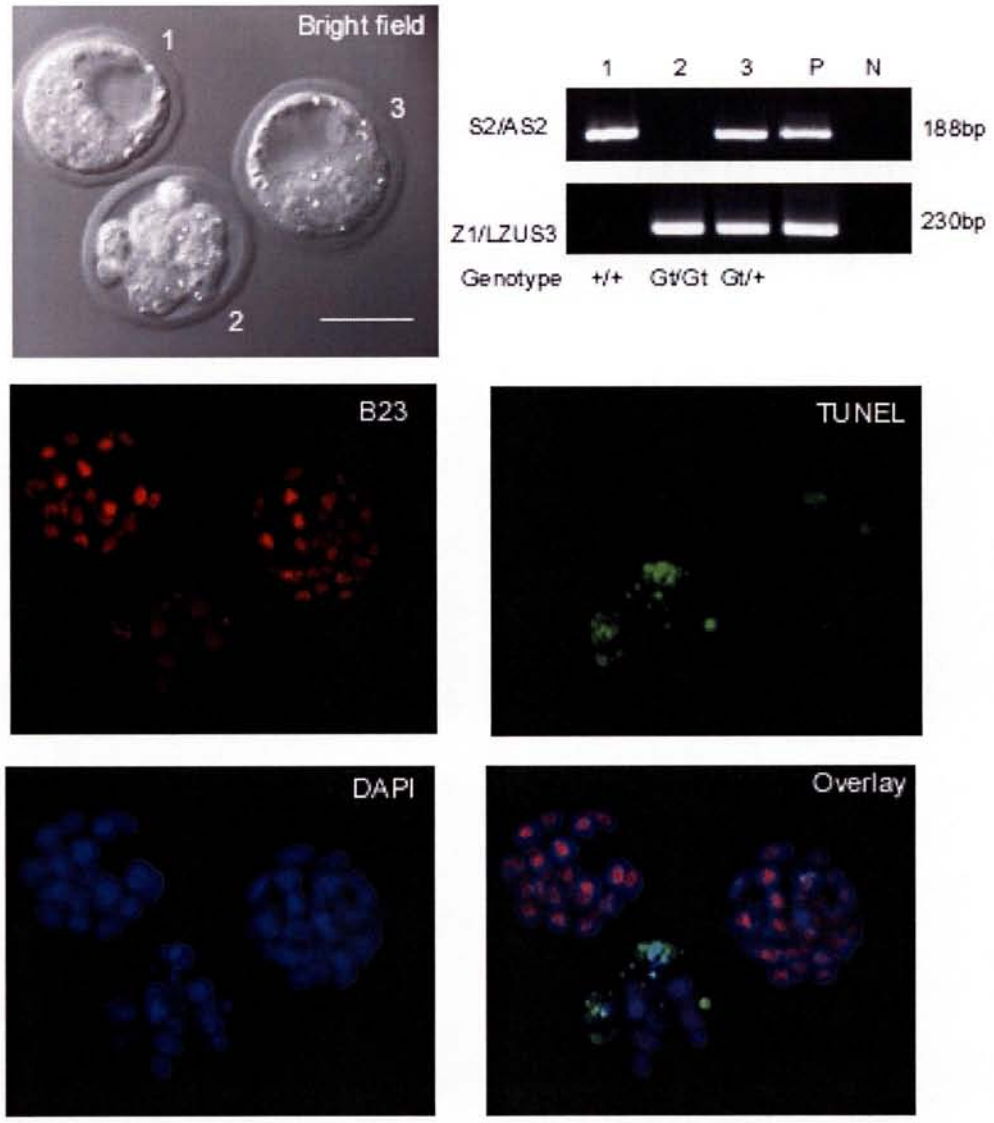

Figure 17. Immuno-histochemical analysis of 3.5 dpc embryos from Rpo1-2$^{Gt/+}$ intercrosses.

Immuno-fluorescence staining with anti-B23/NPM (red), TUNEL staining (green), and nuclear staining with DAPI (blue) of embryos at 94h post hCG. Individually numbered embryos, shown in the bright field photo, correspond to the numbered genotyping results (lower right). Genotypes judged from the PCR are shown under the each lane. P, positive control used with genomic DNA of Rpo1-2$^{Gt/+}$ embryos. N, negative control used with H_2O. Scale bar = 50 μm.

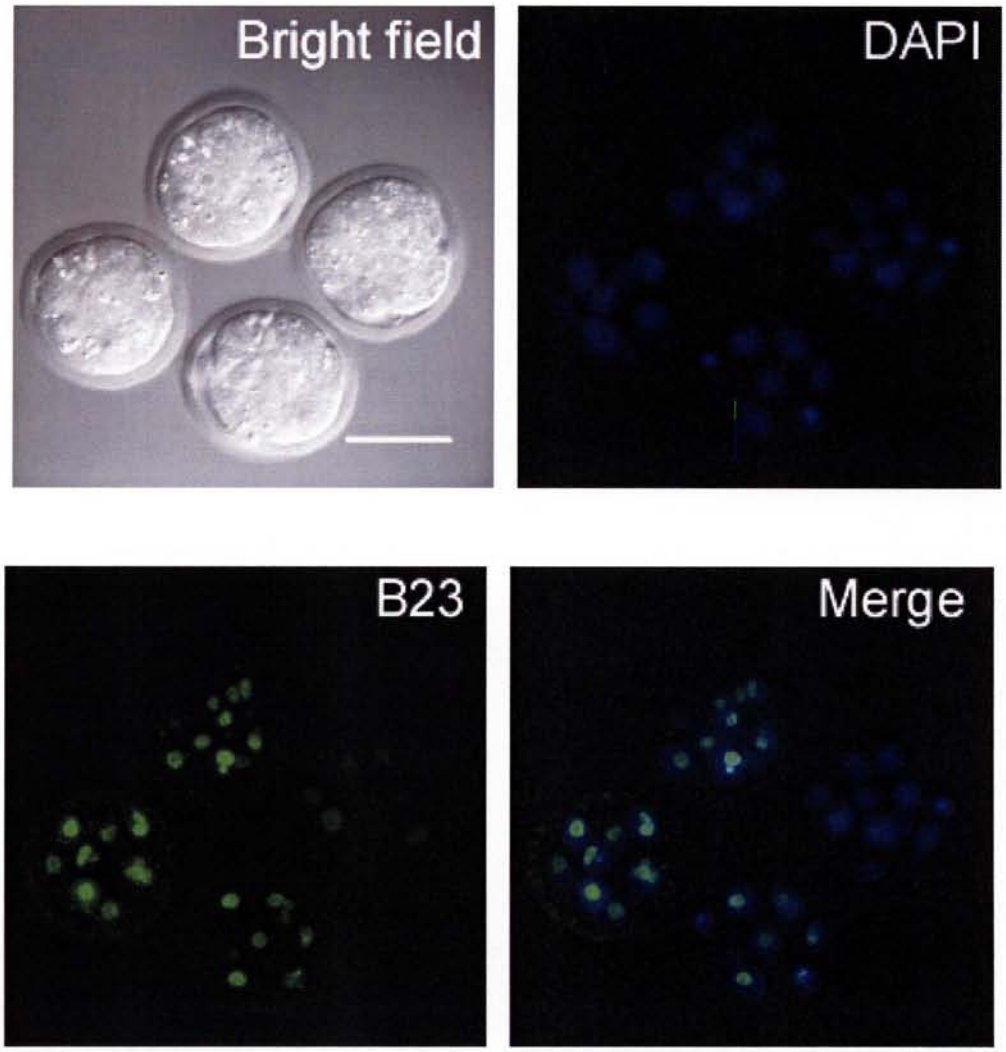

Figure 18. Immuno-histochemical analysis of morulae from Rpo1-2$^{Gt/+}$ intercrosses.

Typical result of immuno-fluorescence staining with anti-B23/NPM (green) and nuclear staining with DAPI (blue) of morphologically normal morulae. Scale bar = 50 μm.

Discussion

Importance of C-terminal domain of Rpo1-2 protein

Although many works have been done on RNA polymerases, most of them are done using the yeast. We reported a gene-trapped mutation of mouse RNA polymerase I subunit.

We have shown that the truncated mutation of the *Rpo1-2* gene resulted in depletion of rRNA and developmental arrest before blastocyst stage. Although we did not confirm the existence of truncated protein due to no available antibody for Rpo1-2 protein, it is highly expected that the truncated Rpo1-2 protein is translated from the fusion mRNA. The deleted C-terminal part of Rpo1-2 protein is the most extensively conserved among different organisms (Shematorova and Shpakovski, 2002), implying their functional and structural importance. According to crystal structure analysis of yeast RNA polymerase II subunits (Cramer et al., 2001), the deleted region contains two domains: One is "hybrid binding" domain (Riva et al., 1987) which binds the nascent RNA strand/template DNA strand as well as the metal (Mg^{2+}) ion at the active site of the largest subunit, and the other is "anchor and clamp" domain which contains a zinc-binding motif and interacts with the clamp domain of the largest subunit (Fig. 19). In addition, a screening of yeast RNA polymerase II mutation showed single amino acid substitution around the zinc binding domain induced lethal phenotype (Scafe et al., 1990; Treich et al., 1991). Therefore, it is expected that the truncated protein cannot function normally.

Existence of maternally inherited mRNA of the *Rpo1-2* gene

On the other hand, we detected very faint band in RT-PCR detecting pre-rRNA synthesis in *Rpo1-2*$^{Gt/Gt}$ embryos, suggesting that RNA synthesis was not abolished completely. One possible explanation is that the truncated protein still retains limited activity for RNA

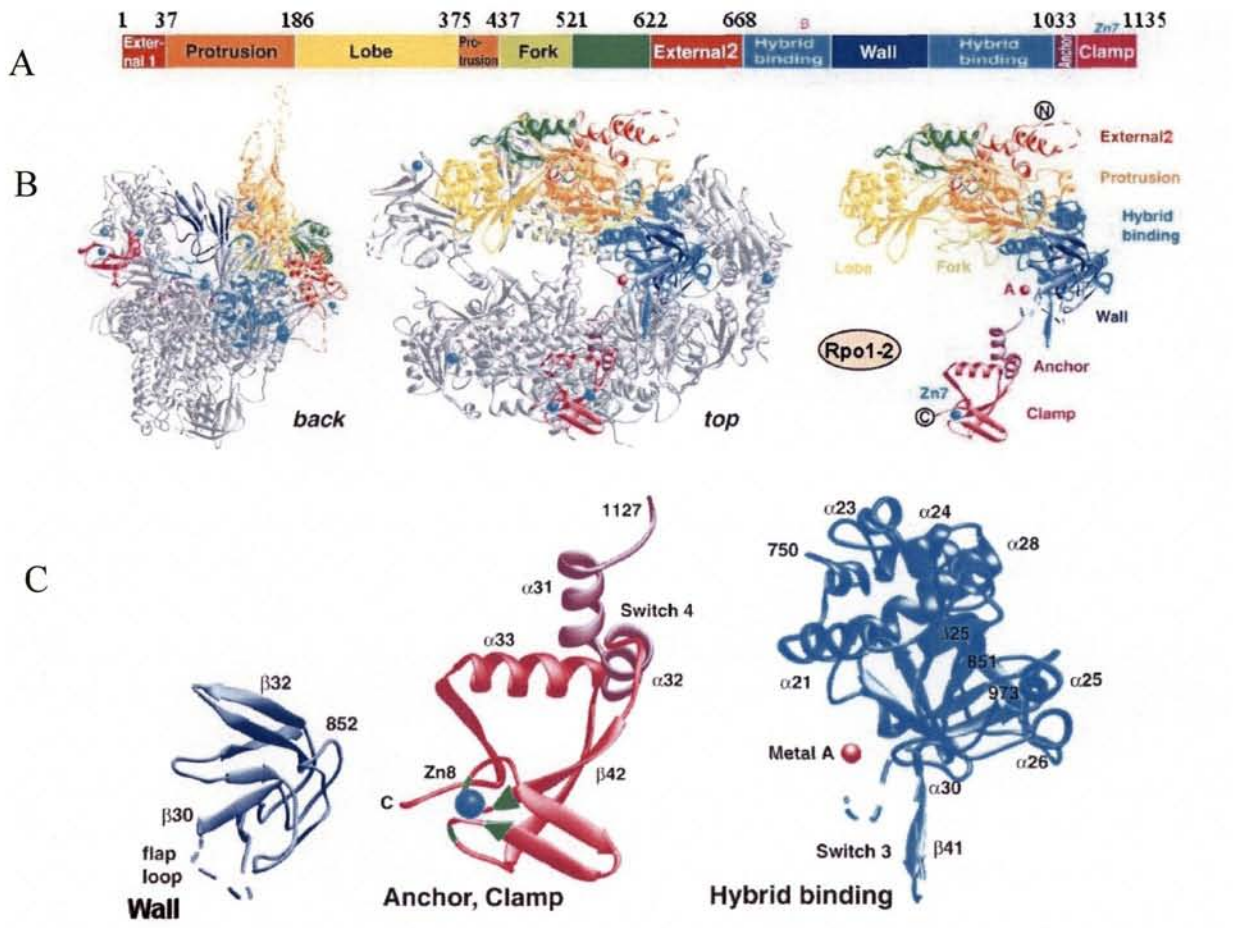

Figure 19. Structure of Rpo1-2 and deleted domain.

(A) Domain and domian like region of Rpo1-2. The amino acid residue numbers at the domain boundaries are indicated. (B) Ribbon diagrams, showing the location of Rpo1-2 within Pol I [Back and top view of the enzyme], and Rpo1-2 alone. Locations of NH2- and COOH-termini are indicated. Color-coding as in (A). (C) Views of domains in Rpo1-2 C-terminal that deleted in Rpo1-2Gt. Half of wall, and half of hybrid binding domain, and anchor-clamp domain were deleted.

synthesis. However, we would like to consider the other possibility, which is existence of maternally inherited mRNA of the *Rpo1-2* gene. Zatsepina *et al* (Zatsepina et al., 2000) reported that maternal Rpo1-2 protein is degraded at metaphase II and that the re-initiation of rRNA synthesis requires *de novo* synthesis and assembly of RNA pol I complex (Zatsepina et al., 2003). Although it is not known whether Rpo1-2 mRNA is maternally inherited in fertilized eggs, we speculate that small amounts of Rpo1-2 protein may be translated from maternally inherited Rpo1-2 mRNA and that this pool of maternal Rpo1-2 mRNA becomes depleted before the blastocyst stage, resulting in the morula arrest phenotype. Similar phenotypes, of pre-implantation lethality, before the blastocyst stage were observed in knockout mice or in knockdown embryos of genes involved in ribosome biogenesis: *Pescadillo* (Lerch-Gaggl et al., 2002), *fibrillarin* (Newton et al., 2003) and *Surf6* (Romanova et al., 2006b). In addition, Baran et al (Baran et al., 2003) reported that mouse embryos treated with actinomycin-D, an inhibitor of Pol I transcription, showed fragmentation of nucleoli, apoptotic nuclei and decrease of cell proliferation at 8-cell to morula stage. From all these results, we speculate that the truncated Rpo1-2 protein does not possess transcription function and that the weak pre-rRNA synthesis activity in *Rpo1-2*$^{Gt/Gt}$ embryos is derived from maternally inherited mRNA of the *Rpo1-2* gene.

Limited amount of Pol I is active for transcription.

In *Rpo1-2*$^{Gt/+}$ mouse, although the *Rpo1-2* mRNA level was nearly half reduced than wild type mouse, the rRNA synthesis was not affected. In many knockout experiments, decreased mRNA level frequently results in decreased protein and activity level. Therefore, in *Rpo1-2*$^{Gt/+}$ mouse, the amount of Rpo1-2 protein is also expected to be decreased. The reason why the total rRNA amount was unchanged in *Rpo1-2*$^{Gt/+}$ mouse may be explained by activity control mechanism of Pol I. Because the regulation of ribosome number is critical for cell

growth and proliferation, transcription of rDNA by Pol I is efficiently regulated in response to changes in growth factors, drugs, stress, or nutrient availability (Grummt, 2003). A key regulator of Pol I transcription apparatus is the transcription initiation factor TIF-IA, the mammalian homolog of yeast RRN3 (Bodem et al., 2000). Biochemical analyses of cell-free transcription systems for Pol I from *Acanthamoeba* (Bateman and Paule, 1986), mouse (Tower and Sollner-Webb, 1987) and yeast (Milkereit et al., 1997) have identified at least two different forms of polymerase, only one of which is able to initiate at the rDNA promoter. Initiation-competent Pol I is less than 2% of total, whereas the bulk of Pol I existed as inactive monomers or dimmers (Milkereit and Tschochner, 1998), and the active Pol I is in stable association with the essential initiation factor RRN3, whose structural and functional homolog in mouse is TIF-IA (Fig. 4) (Bodem et al., 2000). TIF-IA is phosphorylated at multiple sites by a complex network of protein kinases. Thus, the rRNA transcription activity is controlled through phosphorylation of TIF-IA.

Nucleolus in pre-implantation embryos and its stress sensor activity

During the development of pre-implantation mouse embryos, the characteristic nucleolus is not present, but NPBs are formed. NPBs are considered as a structural support for building functional nucleoli in early mammalian development. NPBs are heterogeneous in their ability to recruit rRNA at the 2-4 cell stages (Romanova et al., 2006a; Zatsepina et al., 2003). From the 8-cell stage, all NPBs become active for rRNA transcription and processing, indicating that NPBs of this stage could be considered as functional nucleoli (Zatsepina et al., 2003).

Rpo1-2$^{Gt/Gt}$ embryos displayed NPBs disruption and positive for TUNEL staining, indicating they died for apoptosis. There are many studies presenting that disintegration of nucleolar structure induces apoptosis, and it has been proposed that nucleolus is some sort of stress sensor that monitors ribosomal biogenesis and regulates p53 levels. The apoptosis in response

to nucleolar disruption is most likely due to stabilization of p53 (Olson, 2004; Pestov et al., 2001; Rubbi and Milner, 2003). In normal cell growth conditions, p53 protein levels are kept low by the negative regulator of p53 stability, MDM2/HDM2 protein, which has E3 ligase activity and targets p53 for proteasomal degradation (Ljungman, 2000). Suppression of ribosome biogenesis or a general perturbation of nucleolar function induced to release ribosomal proteins which bind to MDM2 and disrupt the p53-MDM2 complex, resulting in stabilization of p53 (Bhat et al., 2004; Dai et al., 2004; Jin et al., 2004; Lohrum et al., 2003; Zhang et al., 2003). All these experiments are done on somatic cells, when the NPBs can display the stress sensor function is still unclear. Therefore, from our result, it is clear that when NPBs become active for rRNA transcription and processing, the nucleolar stress sensor function would also become active.

Conclusion

1. The pU-Hachi trap vector was inserted in the 14th exon of the *Rpo1-2* gene.
2. A 7.5kb fusion mRNA was transcribed from the trap allele in the heterozygous mouse. The expression of fusion mRNA can be detected from 4-cell stage embryos.
3. The heterozygous mouse was healthy with no apparent phenotype.
4. *Rpo1-2*$^{Gt/Gt}$ embryos failed to develop into blastocyst. They arrested at morula stage and then degenerated.
5. In morula stage *Rpo1-2*$^{Gt/Gt}$ embryos, the pre-rRNA synthesis was severely impaired and immunofluorescence staining result showed the nucleoli were disrupted.
6. The *Rpo1-2*$^{Gt/Gt}$ embryos are strong TUNEL positive in 3.5 dpc, which means they died of apoptosis.
7. It is clear that although only one-fourth in the C-terminal of Rpo1-2 was truncated, the protein can not function normally.
8. Our data also suggests that when NPBs become active for rRNA transcription and processing, the nucleolar stress sensor function also become active.

References

Araki K, Araki M, Yamamura KI. 1997. Targeted integration of DNA using mutant lox sites in embryonic stem cells. Nucleic Acids Res 25(4):868-872.

Araki K, Imaizumi T, Sekimoto T, Yoshinobu K, Yoshimuta J, Akizuki M, Miura K, Araki M, Yamamura K. 1999a. Exchangeable gene trap using the Cre/mutated lox system. Cell Mol Biol 45(5):737-750.

Araki K, Imaizumi T, Sekimoto T, Yoshinobu K, Yoshimuta J, Akizuki M, Miura K, Araki M, Yamamura K. 1999b. Exchangeable gene trap using the Cre/mutated lox system. Cell Mol Biol (Noisy-le-grand) 45(5):737-750.

Baran V, Fabian D, Rehak P, Koppel J. 2003. Nucleolus in apoptosis-induced mouse preimplantation embryos. Zygote 11(03):271-283.

Bateman E, Paule MR. 1986. Regulation of eukaryotic ribosomal RNA transcription by RNA polymerase modification. Cell 47(3):445-450.

Bhat KP, Itahana K, Jin A, Zhang Y. 2004. Essential role of ribosomal protein L11 in mediating growth inhibition-induced p53 activation. The EMBO journal 23(12):2402-2412.

Bodem J, Dobreva G, Hoffmann-Rohrer U, Iben S, Zentgraf H, Delius H, Vingron M, Grummt I. 2000. TIF-IA, the factor mediating growth-dependent control of ribosomal RNA synthesis, is the mammalian homolog of yeast Rrn3p. EMBO Reports 1(2):171-175.

Bonaldo P, Chowdhury K, Stoykova A, Torres M, Gruss P. 1998. Efficient gene trap screening for novel developmental genes using IRES beta geo vector and in vitro preselection. Exp Cell Res 244(1):125-136.

Bradley A, Evans M, Kaufman MH, Robertson E. 1984. Formation of germ-line chimaeras from embryo-derived teratocarcinoma cell lines. Nature 309(5965):255-256.

Chan PK, Qi Y, Amley J, Koller CA. 1996. Quantitation of the nucleophosmin/B23-translocation using imaging analysis. Cancer Lett 100(1-2):191-197.

Chowdhury K, Bonaldo P, Torres M, Stoykova A, Gruss P. 1997. Evidence for the stochastic integration of gene trap vectors into the mouse germline. Nucleic Acids Res 25(8):1531-1536.

Colombo E, Bonetti P, Lazzerini Denchi E, Martinelli P, Zamponi R, Marine JC, Helin K, Falini B, Pelicci PG. 2005. Nucleophosmin is required for DNA integrity and p19Arf protein stability. Mol Cell Biol 25(20):8874-8886.

Cramer P, Bushnell DA, Kornberg RD. 2001. Structural basis of transcription: RNA polymerase II at 2.8 angstrom resolution. Science 292(5523):1863-1876.

Dai MS, Zeng SX, Jin Y, Sun XX, David L, Lu H. 2004. Ribosomal protein L23 activates p53 by inhibiting MDM2 function in response to ribosomal perturbation but not to translation inhibition. Molecular and cellular biology 24(17):7654-7668.

Erbach GT, Lawitts JA, Papaioannou VE, Biggers JD. 1994. Differential growth of the mouse preimplantation embryo in chemically defined media. Biol Reprod 50(5):1027-1033.

Evans MJ, Kaufman MH. 1981. Establishment in culture of pluripotential cells from mouse embryos. Nature 292(5819):154-156.

Friedrich G, Soriano P. 1991. Promoter traps in embryonic stem cells: a genetic screen to identify and mutate developmental genes in mice. Genes Dev 5(9):1513-1523.

Frohman MA, Dush MK, Martin GR. 1988. Rapid Production of Full-Length cDNAs from Rare Transcripts: Amplification Using a Single Gene-Specific Oligonucleotide Primer. Proceedings of the National Academy of Sciences 85(23):8998-9002.

Geiduschek EP, Bartlett MS. 2000. Engines of gene expression. Nat Struct Biol 7(6):437-439.

Ghattas IR, Sanes JR, Majors JE. 1991. The encephalomyocarditis virus internal ribosome entry site allows efficient coexpression of two genes from a recombinant provirus in cultured cells and in embryos. Mol Cell Biol 11(12):5848-5859.

Grummt I. 2003. Life on a planet of its own: regulation of RNA polymerase I transcription in the nucleolus. Genes Dev 17(14):1691-1702.

Hozak P, Cook PR, Schofer C, Mosgoller W, Wachtler F. 1994. Site of transcription of ribosomal RNA and intranucleolar structure in HeLa cells. J Cell Sci 107(2):639-648.

Jang SK, Wimmer E. 1990. Cap-independent translation of encephalomyocarditis virus RNA: structural elements of the internal ribosomal entry site and involvement of a cellular 57-kD RNA-binding protein. Genes Dev 4(9):1560-1572.

Jin A, Itahana K, O'Keefe K, Zhang Y. 2004. Inhibition of HDM2 and Activation of p53 by Ribosomal Protein L23. Mol Cell Biol 24(17):7669-7680.

Kang HM, Kang NG, Kim DG, Shin HS. 1997. Dicistronic tagging of genes active in embryonic stem cells of mice. Mol Cells 7(4):502-508.

Lerch-Gaggl A, Haque J, Li J, Ning G, Traktman P, Duncan SA. 2002. Pescadillo Is Essential for Nucleolar Assembly, Ribosome Biogenesis, and Mammalian Cell Proliferation. J Biol Chem 277(47):45347-45355.

Ljungman M. 2000. Dial 9-1-1 for p53: mechanisms of p53 activation by cellular stress. Neoplasia (New York, NY 2(3):208-225.

Lohrum MAE, Ludwig RL, Kubbutat MHG, Hanlon M, Vousden KH. 2003. Regulation of HDM2 activity by the ribosomal protein L11. Cancer Cell 3(6):577-587.

Long EO, Dawid IB. 1980. Repeated genes in eukaryotes. Annu Rev Biochem 49:727-764.

Mayer C, Grummt I. 2005. Cellular stress and nucleolar function. Cell Cycle 4(8):1036-1038.

Milkereit P, Schultz P, Tschochner H. 1997. Resolution of RNA polymerase I into dimers and monomers and their function in transcription. Biol Chem 378(12):1433-1443.

Milkereit P, Tschochner H. 1998. A specialized form of RNA polymerase I, essential for initiation and growth-dependent regulation of rRNA synthesis, is disrupted during transcription. EMBO J 17(13):3692-3703.

Miller G, Panov KI, Friedrich JK, Trinkle-Mulcahy L, Lamond AI, Zomerdijk JC. 2001. hRRN3 is essential in the SL1-mediated recruitment of RNA Polymerase I to rRNA gene promoters. EMBO J 20(6):1373-1382.

Moore PB, Steitz TA. 2002. The involvement of RNA in ribosome function. Nature 418(6894):229-235.

Moss T. 2004. At the crossroads of growth control; making ribosomal RNA. Curr Opin Genet Dev 14(2):210-217.

Mountford PS, Smith AG. 1995. Internal ribosome entry sites and dicistronic RNAs in mammalian transgenesis. Trends Genet 11(5):179-184.

Newton K, Petfalski E, Tollervey D, Caceres JF. 2003. Fibrillarin is essential for early development and required for accumulation of an intron-encoded small nucleolar RNA in the mouse. Mol Cell Biol 23(23):8519-8527.

Niwa H, Araki K, Kimura S, Taniguchi S-i, Wakasugi S, Yamamura K-i. 1993. An Efficient Gene-Trap Method Using Poly A Trap Vectors and Characterization of Gene-Trap Events. J Biochem (Tokyo) 113(3):343-349.

Nomura M. 2001. Ribosomal RNA genes, RNA polymerases, nucleolar structures, and synthesis of rRNA in the yeast Saccharomyces cerevisiae. Cold Spring Harb Symp Quant Biol 66:555-565.

Olson MO. 2004. Sensing cellular stress: another new function for the nucleolus? Sci STKE 2004(224):pe10.

Olson MO, Hingorani K, Szebeni A. 2002. Conventional and nonconventional roles of the nucleolus. Int Rev Cytol 219:199-266.

Pestov DG, Strezoska Z, Lau LF. 2001. Evidence of p53-Dependent Cross-Talk between Ribosome Biogenesis and the Cell Cycle: Effects of Nucleolar Protein Bop1 on G1/S Transition. Mol Cell Biol 21(13):4246-4255.

Riva M, Schaffner AR, Sentenac A, Hartmann GR, Mustaev AA, Zaychikov EF, Grachev MA. 1987. Active site labeling of the RNA polymerases A, B, and C from yeast. J Biol Chem 262(30):14377-14380.

Romanova L, Korobova F, Noniashvilli E, Dyban A, Zatsepina O. 2006a. High resolution mapping of ribosomal DNA in early mouse embryos by fluorescence in situ hybridization. Biol Reprod 74(5):807-815.

Romanova LG, Anger M, Zatsepina OV, Schultz RM. 2006b. Implication of nucleolar protein SURF6 in ribosome biogenesis and preimplantation mouse development. Biol Reprod 75(5):690-696.

Rubbi CP, Milner J. 2003. Disruption of the nucleolus mediates stabilization of p53 in response to DNA damage and other stresses. EMBO J 22(22):6068-6077.

Scafe C, Martin C, Nonet M, Podos S, Okamura S, Young RA. 1990. Conditional mutations occur predominantly in highly conserved residues of RNA polymerase II subunits. Mol Cell Biol 10(3):1270-1275.

Seither P, Grummt I. 1996. Molecular Cloning of RPA2, the Gene Encoding the Second Largest Subunit of Mouse RNA Polymerase I. Genomics 37(1):135-139.

Shematorova EK, Shpakovski GV. 2002. Structure and Functions of Eukaryotic Nuclear DNA-Dependent RNA Polymerase I. Mol Biol 36(1):1-17.

Shimada H, Kaname T, Suzuki M, Hitoshi Y, Araki K, Imaizumi T, Yamamura KI. 1999. Comparison of ES cell fate in sandwiched aggregates and co-cultured aggregates during blastocyst formation by monitored GFP expression. Mol Reprod Dev 52(4):376-382.

Song CZ, Hanada K, Yano K, Maeda Y, Yamamoto K, Muramatsu M. 1994. High conservation of subunit composition of RNA polymerase I(A) between yeast and mouse and the molecular cloning of mouse RNA polymerase I 40- kDa subunit RPA40. J Biol Chem 269(43):26976-26981.

Stanford WL, Cohn JB, Cordes SP. 2001. Gene-trap mutagenesis: past, present and beyond. Nat Rev Genet 2(10):756-768.

Stoykova A, Chowdhury K, Bonaldo P, Torres M, Gruss P. 1998. Gene trap expression and mutational analysis for genes involved in the development of the mammalian nervous system. Dev Dyn 212(2):198-213.

Strezoska Z, Pestov DG, Lau LF. 2000. Bop1 is a mouse WD40 repeat nucleolar protein involved in 28S and 5.8S rRNA processing and 60S ribosome biogenesis. Mol Cell Biol 20(15):5516-5528.

Sweetser D, Nonet M, Young RA. 1987. Prokaryotic and Eukaryotic RNA Polymerases Have Homologous Core Subunits. Proceedings of the National Academy of Sciences 84(5):1192-1196.

Tower J, Sollner-Webb B. 1987. Transcription of mouse rDNA is regulated by an activated subform of RNA polymerase I. Cell 50(6):873-883.

Treich I, Riva M, Sentenac A. 1991. Zinc-binding subunits of yeast RNA polymerases. J Biol Chem 266(32):21971-21976.

Ulrich Scheer RB. 1990. Functional and dynamic aspects of the mammalian nucleolus. Bioessays 12(1):14-21.

Voss AK, Thomas T, Gruss P. 1998. Efficiency assessment of the gene trap approach. Dev Dyn 212(2):171-180.

Yagi T, Tokunaga T, Furuta Y, Nada S, Yoshida M, Tsukada T, Saga Y, Takeda N, Ikawa Y, Aizawa S. 1993. A Novel ES Cell Line, TT2, with High Germline-Differentiating Potency. Anal Biochem 214(1):70-76.

Yuan X, Zhou Y, Casanova E, Chai M, Kiss E, Grone HJ, Schutz G, Grummt I. 2005. Genetic inactivation of the transcription factor TIF-IA leads to nucleolar disruption, cell cycle arrest, and p53-mediated apoptosis. Mol Cell 19(1):77-87.

Zatsepina O, Baly C, Chebrout M, Debey P. 2003. The step-wise assembly of a functional nucleolus in preimplantation mouse embryos involves the cajal (coiled) body. Dev Biol 253(1):66-83.

Zatsepina OV, Bouniol-Baly C, Amirand C, Debey P. 2000. Functional and Molecular Reorganization of the Nucleolar Apparatus in Maturing Mouse Oocytes. Dev Biol 223(2):354-370.

Zhang Y, Wolf GW, Bhat K, Jin A, Allio T, Burkhart WA, Xiong Y. 2003. Ribosomal Protein L11 Negatively Regulates Oncoprotein MDM2 and Mediates a p53-Dependent Ribosomal-Stress Checkpoint Pathway. Mol Cell Biol 23(23):8902-8912.